Energy & Buildings 173 (2018) 221–238

Contents lists available at ScienceDirect

Energy & Buildings

journal homepage: www.elsevier.com/locate/enbuild

Ground truthing the environmental benefits of a polygeneration system: When to combine heat and power?

Peter Berrill*, Edgar G. Hertwich

Center for Industrial Ecology, Yale School of Forestry and Environmental Studies, New Haven, USA

ARTICLE INFO

Article history:
Received 24 January 2018
Revised 23 April 2018
Accepted 7 May 2018
Available online 27 May 2018

ABSTRACT

Energy systems are major contributors to critical environmental problems including climate change and air pollution. Over half of global energy end use is in the form of heat, three-quarters of which is from fossil fuels. We assess different ways to provide heat, cooling, and electricity to a university campus, comparing lifecycle primary energy requirements, greenhouse gas (GHG) emissions, and particulate matter impacts. For this case study, replacing cogeneration of cooling, heat, and power with grid electricity and building level heating and cooling can reduce GHG emissions by 30%, while cogeneration of heating and cooling in an electrically powered heat recovery chiller system with thermal energy storage can reduce GHG emissions by 45%. GHG reductions from grid electricity remain even if it is assumed to come from more carbon intensive marginal electricity generation. Prominent factors affecting the environmental benefits of polygeneration are identified, most notably the fuel mix and energy efficiency of regional grid electricity, and combined heat and power system efficiency. Thermal energy storage adds resilience to the system while reducing environmental impacts. A heuristic charts the viability of combined versus separate heat and power production for a general case, based on cogeneration efficiency and regional electricity carbon intensity. Low carbon grid electricity strengthens the case for a shift in polygeneration systems from combined heat and power to combined heating and cooling.

1. Introduction

In the light of recent climate agreements and ambitious climate goals, actors at subnational levels such as states [1], cities [2] and institutions [3] are pledging to reduce greenhouse gas (GHG) emissions in order to help to achieve or surpass national targets. A central component of such pledges are energy systems; reducing consumption via energy efficiency, and switching to less polluting fuels and conversion technologies where possible. Of the main energy carriers (i.e. electricity and combustion fuels) used by end users, electricity is easiest to decarbonize in the short term, as low-carbon technologies are available and increasingly competitive. But electricity accounts for just 18% of *final energy consumption* globally, with oil representing 41%, natural gas 15%, and coal 11% [4,5]. Even if we transformed to a zero-carbon electricity system tomorrow, over 75% of greenhouse gas emissions would remain [6]. Decarbonizing electricity will have a broader impact if end uses such as transport and heating become increasingly electrically powered, but focusing on electricity alone is insufficient for making serious GHG reductions.

The International Energy Agency reported that in 2011 over half of global final energy consumption was in the form of heat, three-quarters of which was fossil fuel based [7]. Buildings, just above industry, are the biggest heat consumers [7,8]. Space and water heating in buildings have received much attention in energy and environmental literature [9–15]. The demand for heat, for industrial or building use, is often located in close proximity to demands for electricity and/or cooling, presenting opportunities for cogeneration or polygeneration of multiple energy services. Cogeneration of heat and power (CHP) and polygeneration (of heat, power, and usually cooling) systems have been studied for their potential to reduce primary energy use, economic costs and environmental impacts of providing energy services [16,17]. The scale of such generation can be micro level (<50 kW_{el}) for individual houses or a small group of buildings, or meso-level (<50 MW_{el}), from a plant that generates and distributes energy services to large institutional/industrial customers or many small customers providing concentrated demand.

A number of optimization approaches for polygeneration in buildings have been performed, of which Rong and Su provide a recent review [18]. The optimization objective, building function, and system type and scale varies between studies. Selections from the literature include cost optimization of different polygenera-

* Corresponding author.
E-mail address: peter.berrill@yale.edu (P. Berrill).

https://doi.org/10.1016/j.enbuild.2018.05.020
0378-7788/

tion systems for residential buildings in Iran [19], comparison of polygeneration strategies for an office building in Mississippi optimized separately for cost, energy use, and environmental impacts [20], a cost optimization of polygeneration for a university campus in Texas [21], and cost optimizations of a factory [22] and isolated tourist resort [23] in Italy. Other work has used multi-objective optimization to solve simultaneously for economic and energy/environmental objectives, such as a study of polygeneration at a university campus in Japan [24], studies of hospital energy use in Greece [25] and Spain [26], and a study of a mixed-use group of Passivehaus standard buildings in the UK [27].

Several studies use life cycle assessment (LCA) or emission and primary energy use factors from literature to determine primary energy use and environmental performance of co/polygeneration, often in comparison with conventional alternatives [26–37]. LCA has the potential to provide comprehensive comparisons of product and service systems, incorporating resource extraction, transport, manufacturing, use, maintenance, and end of life phases. While most studies report economic benefits from polygeneration, there are mixed conclusions as to the environmental benefits. One case study by Carvalho et al. reported grid power plus separate generation of heating and cooling to perform better in environmental terms than polygeneration for a hospital in Spain [26]. Some studies find the environmental benefits of polygeneration to depend on factors such as the type of electricity generator and percent of full load that it operates at [28], the ratio of cooling to heating load [28,32], or the carbon intensity of grid electricity [34,36]. Studies that found polygeneration to perform better than conventional generation were located in regions with relatively carbon intensive grid electricity; 565 [27], 460–570 [29], 1,230 [30], 705 [33] and 682 [37] $kgCO_2$-eq/MWh respectively.

A strategy to enhance the performance of cogeneration and polygeneration is thermal energy storage (TES), which facilitates greater utilization of the heating and cooling generated, allowing plants to run at a higher capacity factor. Different authors have studied ways to cost optimize polygeneration with TES [21,22,38], however none of these studies incorporate an environmental assessment. Meanwhile, quite little research has been done on strategies to meet simultaneous heating and cooling loads via heat recovery chillers [39,40] or otherwise [41]. Heat recovery chillers (HRC) recover heat removed from a chilled water loop to heat a hot water loop, putting ambient heat removed from cooled spaces to use and enabling very high overall efficiencies for simultaneous heating and cooling. This paper fills a gap in the literature by presenting an LCA of a meso-scale district energy system, comparing two polygeneration alternatives to separate generation of heating, cooling, and electricity. The technology systems are not intended to be exhaustive of possible technical solutions, but offer an instructive comparison of the current polygeneration system to independent generation, and to a different system incorporating combined heating and cooling and thermal energy storage, two understudied promising technologies. Scenarios based on technology and grid electricity characteristics in 2015 and 2030 are compared. The findings offer a ground-truthing of the environmental benefits of CHP, which are shown to depend crucially on system efficiencies and the carbon intensity of grid electricity. The findings demonstrate the great potential of cogenerating heating and cooling to reduce environmental impacts associated with thermal energy services.

2. Case study

The case study analyses the generation and distribution of heating, cooling, and electricity in the Yale University campus over a model year. These energy services are currently generated locally at a campus power plant and chiller plant and distributed among the central campus. The power plant has a generating capacity of 16 MW_{el}, roughly equivalent to the average electricity demand of 16,000 Connecticut homes [42], from two electric-load-following gas turbines. A heat recovery steam generator (HRSG), gas boilers, and compression chillers generate steam and chilled water for campus heating and cooling. Regional grid electricity supplements electricity supply when demand exceeds local generation, and in shoulder[1] seasons when the combined thermal demands are lowest (lowering the utility of steam produced via the HRSG). Input of grid electricity is typically 5–10% of total electricity supply but reaches 25% in the shoulder season months of March and October.

Fig. 1 shows heating, cooling, and electricity demands over a model fiscal year (July – June), based on historical demand. These data can be viewed in the 'CCHP Sum' tab of Data File 1 (DF-1) [43]. Heating degree days (HDD) and cooling degree days (CDD) are shown for each month, relative to a base temperature of 18.3 °C (65°F), based on six-year average (July 2011 – June 2017) readings from New Haven airport [44], about five miles from the campus. HDD and CDD give an indication of heating and cooling requirements, but do not include requirements for humidity control, which are an important determinant of energy use for space conditioning in summer. Electricity demand is stable, while heating and cooling loads vary with the seasons. There are residual heating and cooling demands in the 'off-seasons' with some heating being required in summer and cooling required in winter. Reasons for these off-season demands include humidity control which requires reheat of dehumidified air in the summer, certain spaces (e.g. labs, museums, galleries) with strict temperature and humidity set points, hot water demand, and suboptimal controls. Total cooling and power demands over the course of a year are 112 GWh and 118 GWh, with heating demands approximately 1.5 times larger, at 167 GWh. Three alternative supply systems are described in Section 3 and Fig. 3.

3. Methodology and system descriptions

3.1. Life cycle assessment

The study extends THEMIS [45], an LCA tool with detailed electricity generation inventories. The system boundary includes all processes which extract, transport, generate, store, and distribute energy for each system/scenario. The functional unit is twelve months of demand for electricity, heating, and cooling by a portion of the Yale University campus. Foreground inventory data describing the current polygeneration system, regional grid electricity production (modelled as ISO-New England electricity), gas boilers, compression and heat recovery chillers, and TES are used. Existing data in THEMIS, which incorporates ecoinvent v2.2 [46,47], provide inventories for remaining upstream processes. The energy systems as described in 3.2–3.4 and depicted in Fig. 3a–c are first represented as energy flow tables in the form of a physical input output table (PIOT) in energy units.[2] This PIOT approach facilitates the transformation of production functions to a technical coefficient matrix A consisting of linear input coefficients a_{ij}

$$a_{ij} = z_{ij}/x_j \tag{1}$$

where z_{ij} is the quantity of energy flowing from process i into process j, and x_j is total energy output from process j. Column j of A will describe all inputs required to produced one unit of output j, e.g. the inputs to 1 MWh of campus electricity in July of the CCHP system consist of 0.91 MWh of electricity from the gas turbine, and

[1] The shoulder season refers to an intermediate 'changeover' period between heating and cooling seasons.

[2] We use matrix terminology from hybrid-LCA, consistent with [45], except that we refer to the stressor matrix of emission intensities as S (Eq. (4)), rather than F.

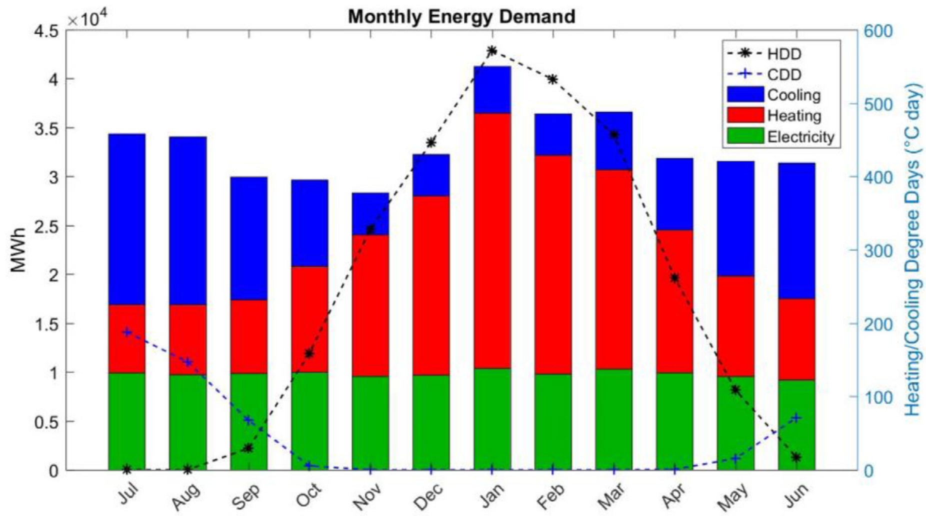

Fig. 1. Monthly demand for electricity, heating, and cooling (MWh) and HDD/CDD (°C-day).

0.09 MWh of electricity from the grid. Total output x_i from each process is calculated as the sum of inputs to other processes z_{ij} and final demand for the product of that process $y_{i\cdot}$.

$$x_i = \sum_j z_{ij} + y_i \tag{2}$$

The PIOTs are constructed for each month of the year, as the demands, operating conditions and efficiencies vary monthly. We recognize that there are demand variations within each month, and that input requirements at can change instantaneously in response to demand. Data at high a temporal resolution can be useful for identifying levels of excess thermal generation, and real-time carbon intensity of regional electricity which varies throughout the day. Such resolution of data was not available for this study, and we consider the monthly time step sufficient to capture seasonal changes in demand and supply throughout a model year. The issues of excess heat generation, thermal storage potential and capacity, and carbon intensity of marginal electricity are discussed further in 3.2, 3.4, and 3.6. The PIOTs for each supply system for each month of the year can be viewed in DF-1 for 2015, and Data File 2 (DF-2) for 2030 [43].

The technical coefficient matrices resulting from the energy PIOTs are appended to THEMIS, moving its functionality beyond analysis of electricity supply systems to analysis of heating, cooling, and electricity supply systems. THEMIS was chosen due to its high resolution in electricity generation technologies, feedbacks between foreground electricity and background production processes [45], and it's up-to-date representation of fugitive emissions from oil and gas extraction [48]. Three alternative supply systems, described in 3.2–3.4, are analyzed under two temporal scenarios with two sensitivity cases.

The monthly final demand vector, y, consisting of demand for heating, cooling, and power (c.f. Fig. 1), is converted into monthly production by all processes to meet that demand, x, via pre-multiplication by the Leontief inverse, L, of the technical coefficient matrix, A. I is an identity matrix with the same dimension as A and L.

$$x = Ly = (I - A)^{-1} y \tag{3}$$

To calculate environmental impacts, d, the production vector x is pre-multiplied by a stressor matrix, S, containing environmental stressors (extractions from and emissions to the environment) per unit production by each process, and a characterization matrix, C, containing Midpoint characterization coefficients from the ReCiPe life cycle impact assessment methodology [49]. Primary energy requirements are calculated using the Cumulative Energy Demand (CED) indicator [49]; this includes all fuel energy input or lost in the extraction and transport of fuels, energy conversion, and plant construction. Renewable resources such as wind and solar energy are not included in CED, but the embodied energy of renewable energy plants is included. Eq. (4) sums up the central equation of matrix-based LCA.

$$d = CSx = CSLy = CS(I - A)^{-1} y \tag{4}$$

Eq. (5) shows impacts $\hat{d}$ based on the diagonalized final demand matrix $\hat{y}$. The diagonalization process transforms a n x 1 column vector y into an n x n matrix $\hat{y}$, with the ith element of y on the corresponding diagonal $(i = j)$ element of $\hat{y}$, and zeros on the off-diagonals.

$$\hat{d} = CSx_y = CSL\hat{y} = CS(I - A)^{-1} \hat{y} \tag{5}$$

This facilitates a contribution analysis whereby impacts associated with individual components of final demand can be calculated. For instance, the demand for 12,540 MWh of cooling in September can be traced back to inputs from CHP electricity, grid electricity, and steam. These inputs can be further traced back to fuel inputs to the CHP, grid electricity, steam, infrastructure inputs, fuel extraction and distribution, etc.

3.2. Combined cooling, heating and power system

We describe the current form of the campus energy plant as a Combined Cooling, Heating, and Power (CCHP) system. A Sankey diagram of current energy inputs to the plant and their conversion into energy services and losses is shown in Fig. 2. Fig. 3a shows a schematic diagram of the main system components. A Sankey diagram of this system with 2030 efficiencies can be viewed in the Appendix (Fig. A1). Natural gas is combusted in a gas turbine to produce most of the electricity needs of the campus, with additional electricity supply coming directly from the regional grid. Flue gas from the gas turbines enters a heat recovery steam generator (HRSG) which converts heat in the flue gas into steam. To boost the steam output of the HRSG, additional natural gas is burned in a duct burner. When heating demands require further steam generation, gas is combusted directly in gas boilers.

A series of compression refrigeration chillers cool water for campus cooling. The chillers run either on steam or electric power

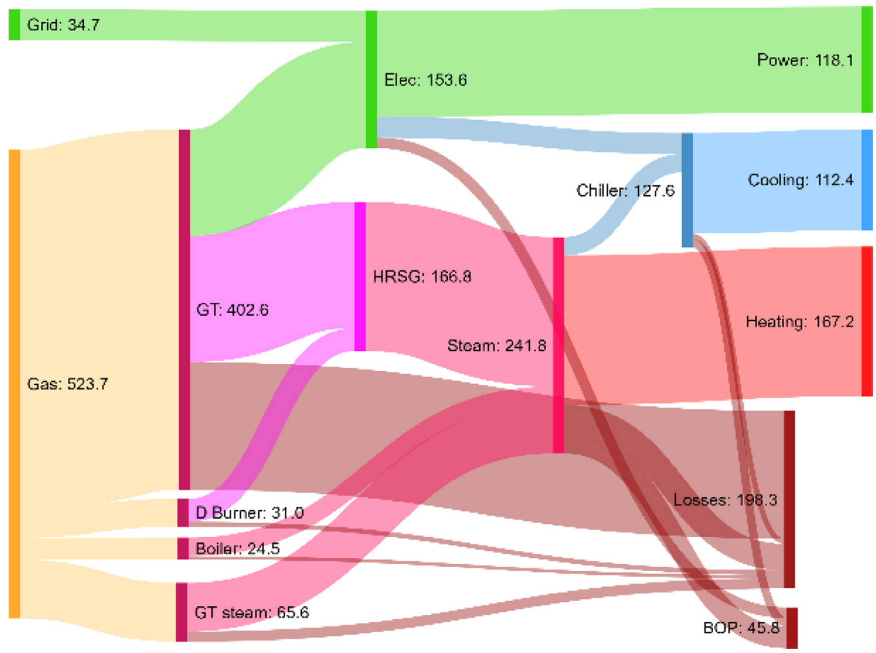

Fig. 2. Sankey diagram of energy flows in the current CCHP system, measured in GWh.
BOP = Balance of Plant; GT = Gas Turbine; D Burner = Duct Burner; HRSG = Heat Recovery Steam Generator.

depending on the season, with excess steam in the summer being used to power the chillers. In the winter, electric power alone powers the chillers. The coefficient of performance (COP) of the chilling process is on average 1.4 when powered by steam (ranging from 1.3–1.7 depending on month and humidity levels) and 4.7 when powered by electricity. In addition to the campus demands for electricity, heating and cooling, the power plant and chiller plant require inputs of all three services for processes and operations to keep the plants running, collectively known as balance of plant (BOP). Venting of excess steam is also accounted in our data source as BOP. BOP varies monthly, constituting 0–8% of total power/heating/cooling output in winter and 7–20% of total output in summer. One reason that BOP is lower in the winter is that lower ambient temperatures can provide 'free' cooling to the cooling towers. Another reason for higher BOP in summer is venting of excess steam to the atmosphere. It is possible that other technologies, such as absorption heat pumps, could utilize this waste heat, but as that would require incorporating additional demands from outside of the campus, such solutions were considered out of scope. We estimate losses from distribution of steam (15%) and chilled water (5%) with assistance from campus energy system engineers and literature [19,50–52]. Upstream grid electricity losses from transmission and distribution are assumed to be 5%, in line with the national average [53]. The direct inputs required are 35 GWh of electricity and 524 GWh of natural gas[3] with 2015 technology, and 25 GWh of electricity and 433 GWh of natural gas with 2030 technology.

3.3. Separate cooling, heating and power system

One alternative to the current supply system, denoted as Separate Cooling, Heating, and Power (SCHP), involves production of each energy service separately, using regional grid electricity to meet all electricity demand, and using natural gas and electricity to produce hot and cold water directly at the building level via small scale boilers and chillers. A schematic diagram describes the SCHP system in Fig. 3b, and Sankey diagrams for 2015 and 2030 can be viewed in the Appendix Fig. A2. Distribution losses are generally smaller for hot water than for steam [52], and in this case as distribution distances are much smaller (hot and cold water are assumed to be generated by boilers and chillers in each building), distribution losses are assumed to be just 1%. We note that changing a distribution system from steam to hot water is not straightforward; the practicalities, impacts, and costs of such a change are outside of the boundary of this analysis, which is intended as a comparison between different generation and distribution systems. The direct inputs required are 147 GWh of electricity and 199 GWh of natural gas in 2015, and 139 GWh of electricity and 188 GWh of natural gas in 2030.

3.4. Separate power, combined heating and cooling system

A second alternative, titled Separate Power with Combined Heating and Cooling (SPCHC) is depicted in Fig. 3c. Electricity is again supplied solely by the grid, while a HRC cogenerates hot and cold water to meet simultaneous heating and cooling loads. With a combined COP of 5.6, 1 kWh of electricity input removes 2.3 kWh from the water being chilled while generating 3.3 kWh of hot water. These operating efficiencies are based on a recently deployed HRC system at Stanford University [51], and are not assumed to improve between 2015 and 2030, although it is possible that this technology could become more efficient. For heating and cooling loads that fall outside the 3.3:2.3 ratio, i.e. when there are additional heating or cooling demands that cannot be supplied by the HRC, regular boilers and chillers make up the residual supply. This alternative supply system also incorporates the possibility of hot and cold TES. This serves as a buffer to maximize the capacity factor of the HRC. We assume that each month, the thermal storage capacity is sufficient to allow the HRC to generate heating and cooling water in the ratio of 3.3:2.3 to the extent that heating and cooling loads allow in each month, ensuring that all heating

[3] The energy content of natural gas input to the system is presented in MWh rather than volumetric or other energy units for ease of comparison with electricity inputs.

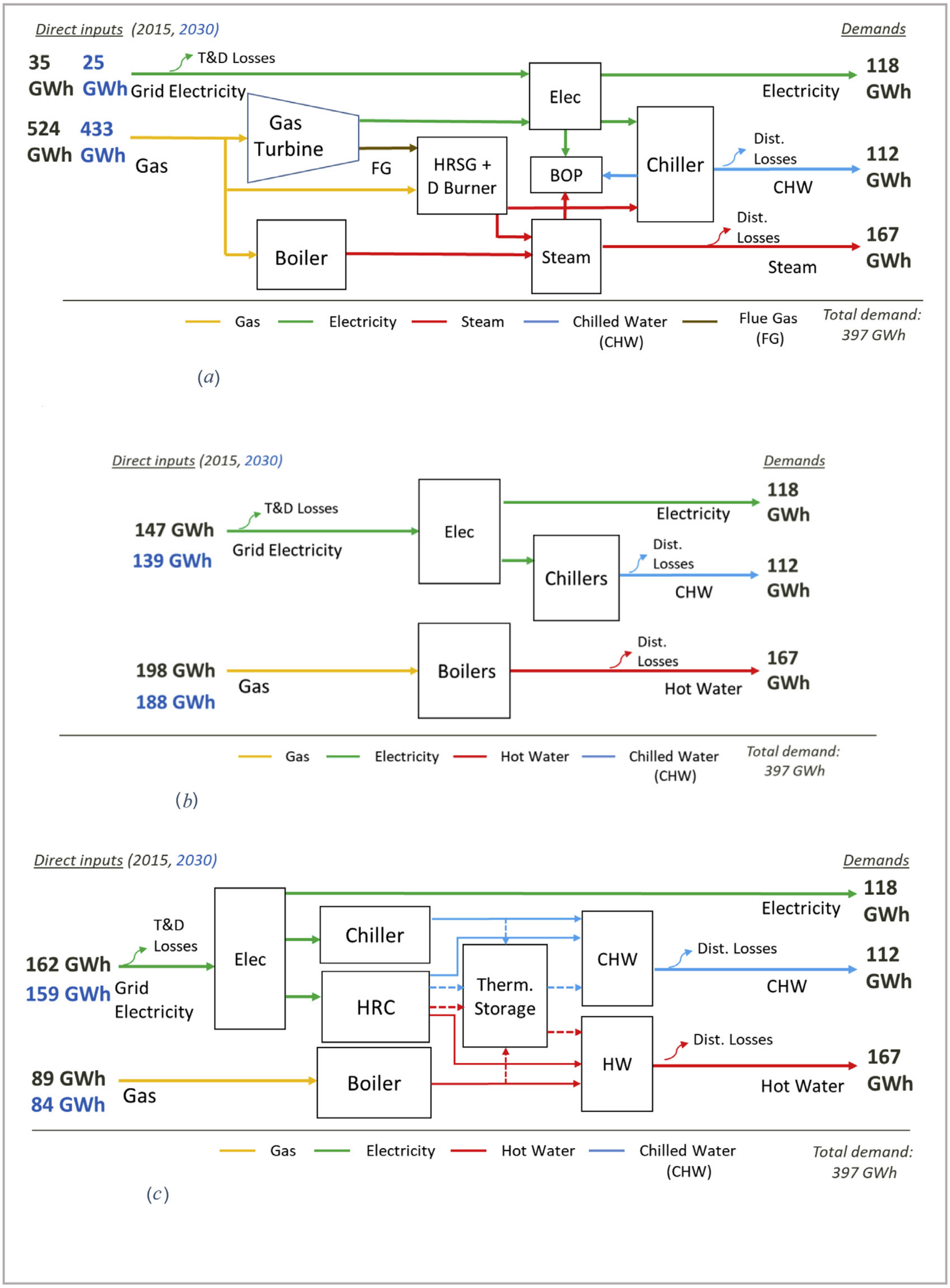

Fig. 3. (a) Schematic diagram of current combined cooling, heat, and power (CCHP) system. BOP = Balance of Plant; HRSG = Heat Recovery Steam Generator; D Burner = Duct Burner; GT = Gas Turbine. (b) Schematic diagram of alternative system 1: separated cooling, heat, and power (SCHP) (c) Schematic diagram of alternative system 2: separate power with combined heating and cooling (SPCHC). HRC = Heat Recovery Chiller; HW = Hot Water.

and cooling from the HRC is used. A simplified sizing of TES tanks is performed, based on an assumption that the capacity should be roughly equal to the average demand for heating and cooling in a single day. See the 'TES Capacity' tab of DF-1 for calculations of capacity of TES infrastructure. Roundtrip energy losses from the TES cycle are not considered. The assumptions of sufficient capacity and no storage energy losses generate a 'best case scenario', or upper bound for the performance of the HRC-TES system.

As hot and cold water are generated centrally in this system, losses associated with hot water and chilled water distribution are assumed to be 5%, consistent with lower losses from hot water versus steam distribution [51,52]. The generation efficiencies of grid electricity [45,54] are inclusive of BOP losses, while BOP

losses from the HRC system are assumed to be negligible. The direct inputs required in 2015 would be 162 GWh of electricity and 89 GWh of natural gas, and 159 GWh of electricity and 84 GWh of natural gas in 2030.

3.5. Allocation

In any process that produces more than one product, or uses another processes' waste as a useful input, there are a number of ways to assign the inputs to, and emissions from, that process to the different products [55,56]. This issue of allocation is familiar to LCA. Inputs and emissions can be allocated based on economic value [57], by some physical characteristic of the products [58], or the avoided burned of producing the co-product can be subtracted [29]. In analyses of energy systems, energy content or exergy content are commonly used as the basis for allocation [31]. Exergy captures the quality of energy flows in a way that energy content does not, and an exergy analysis of heat, cooling and electricity will assign larger impacts to electricity due to electricity's higher exergy content [31,58]. In this analysis, to preserve the consistency of the energy unit PIOT and for simplicity, allocation is based on energy content. A sensitivity is performed where allocation of joint production processes is based on exergy content. This applies only to the CHP-HRSG system of CCHP, and the HRC of SPCHC.

3.6. Scenario definition

For the three supply systems defined above, the analysis is run for two temporal scenarios, one representing 2015 technology and electricity mix, and a future oriented scenario reflecting expected average technology and electricity mix in 2030. This allows us to see how the alternative supply systems compare today and in the future when some system components achieve higher operation efficiencies. For 2015 supply systems, regional grid electricity is modelled using the 2015 monthly average grid mix in ISO-NE [59]. Generation efficiencies match 2015 average performance in USA [54]. One sensitivity analysis is performed where monthly marginal electricity mix in 2015 is used to represent grid electricity inputs, and a second sensitivity analysis uses exergy rather than energy based allocation for multi product processes, as described above. The marginal electricity mix provides a worst case scenario of grid carbon intensity, as it uses higher proportions of oil, coal, and gas. Pumped storage is assumed to be charged with the monthly average mix, with a 90% roundtrip efficiency.

For 2030 the regional electricity grid mix is updated from the current supply mix to expected mix in 2030, based on proposed and forecast capacity additions [60–62]. It is interesting to see that carbon intensity is projected to slightly increase in 2030, due to the retirement of nuclear facilities and insufficiency of renewable capacity additions and natural gas efficiency increases to counteract that (behind-the-meter rooftop solar PV is not included). See the Appendix and the 'ISO-NE Gen Mixes' tab of DF-1 for projection methods and calculation of the 2030 mix. Natural gas plants make up most of proposed capacity additions [62], and we project that efficiency will increase slowly in line with the current rate of efficiency improvement [54], while coal efficiency is assumed to remain constant, as we don't expect newer more efficient coal plants to come online. Monthly average and marginal generation mixes for 2015 are shown in Table S1 and Table S2 of the Appendix. Changes in building efficiency and energy use patterns may lead to different demand and supply of energy services in 2030 [63], but for fairness of comparison the energy demands in the functional unit are not changed between temporal scenarios. Table 1 summarizes technology parameters for the 2015 and 2030 technology scenarios.

4. Results

4.1. Annual impacts

The main results of the analysis are presented in Fig. 4. All results are summarized in tabular form in Appendix Tables A3–A6. We find that for this case study, cogenerating heat and power with periodic utilization of excess steam for cooling is not a solution that uses less primary energy or generates less environmental impacts than separate generation of cooling, heating, and power. Primary energy requirements are 6% (SCHP15) and 17% (SPCHC15) less in two alternatives to the current CCHP system with 2015 average technology (Fig. 4a). Improved efficiency assumptions for 2030 technology changes the primary energy comparison, but total requirements remain comparable between CCHP and SCHP and reduce with SPCHC.

The alternative supply systems bring about greater reductions to carbon footprints (CF) (Fig. 4b). Fuel use and emissions associated with cooling and heating are substantially reduced, while the impact of increased primary energy requirements for grid electricity is more than compensated for by lower carbon inputs to electricity. We see CF reductions of 30% with a SCHP15 supply system and 45% with a SPCHC15 supply system, compared with CCHP15. In 2030, largely due to efficiency improvements in the cogeneration of power and steam, CF reductions compared to CCHP30 are smaller yet still sizeable, 17% for SCHP30 and 32% for SPCHC30.

Particulate matter (PM) impacts follow a similar pattern to CF (Fig. 4c), as both are closely related to the use of natural gas, although the main sources of emissions differ. Most PM impacts arise from SO_2 releases during natural gas extraction, while GHG emissions are predominantly from natural gas combustion, although CH_4 releases during extraction are important contributors. Freshwater ecotoxicity (FET) impacts (Fig. A4) are also strongly linked with natural gas extraction, and are considerably smaller in SCHP and SPCHC systems than CCHP. In our sensitivity analysis using marginal rather than average grid electricity in 2015, total emission reductions from alternative systems are diminished but still notable: e.g. GHG emissions are reduced 12% for the SCHP15m system, and 24% for the SPCHC15m system (Appendix Fig. A7; Table A4). In our sensitivity analysis using exergy allocation, total impacts do not change, but the allocation of impacts between final uses changes (Fig. A8).

4.2. Monthly impacts

A monthly breakdown of GHG emissions for the three supply systems using 2015 technology is shown in Fig. 4 (d – f) reflecting not only varying energy demands, but also varying system performance and monthly average grid mix. Reduced emissions from cooling are evident in the summer months for both SCHP15 and SPCHC15 compared to CCHP15, as a result of switching from partially steam-powered cooling to lower carbon intensity and more efficient electric-powered cooling. Heating related emission reductions in SCHP15 are evident in all months. Cogeneration of heating and cooling by the HRC in the SPCHC15 system enables considerable reductions in heating emissions compared to SCHP15, especially in the warmest months (May-Oct). Monthly primary energy requirements for 2015 are shown in Appendix Fig. A5.

4.3. Impact intensities

The carbon intensities of heating, cooling, and electricity are shown in Fig. 5 for the current CCHP15 system and the SPCHC15 alternative system for three months of the year; the maximum cooling month (July), maximum heating month (January) and a

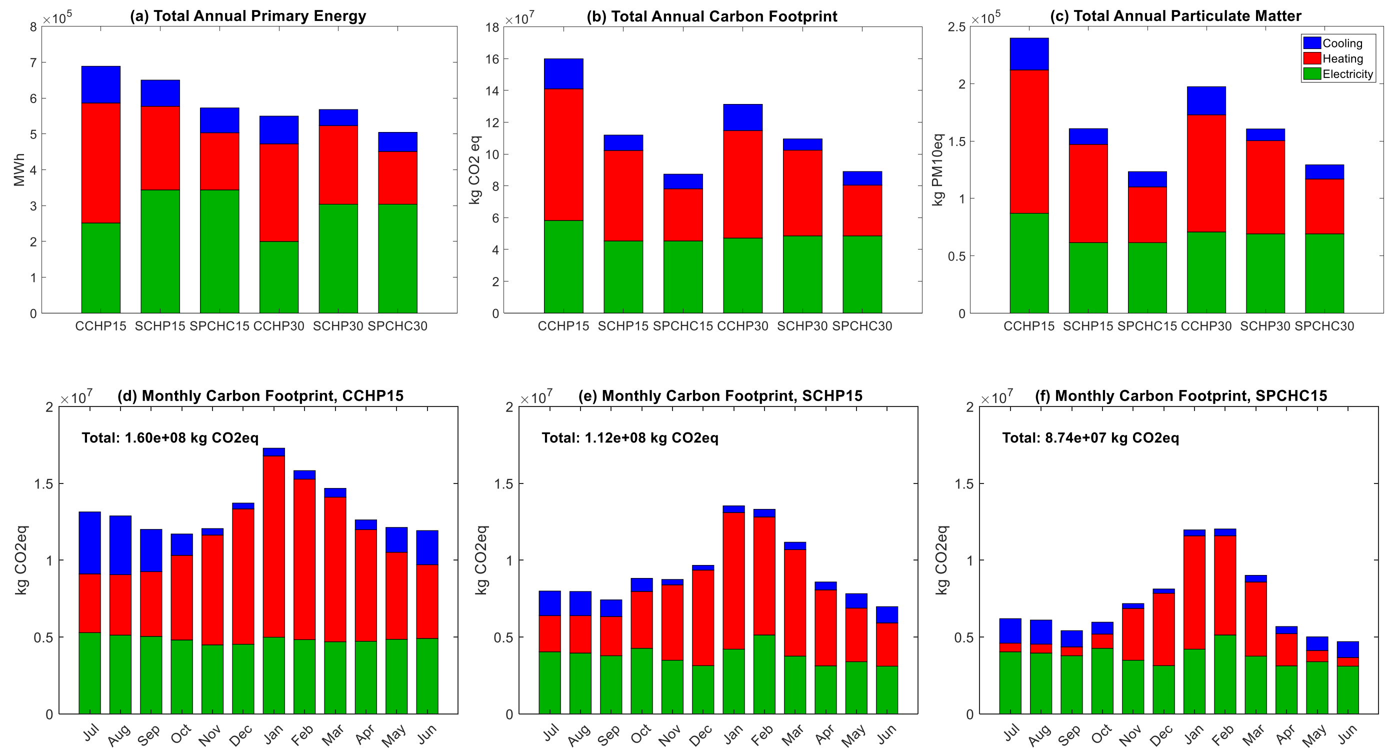

Fig. 4. Total annual Primary Energy requirements (a), Carbon Footprint (b) and Particulate Matter (c) impacts for the current system and two alternatives with 2015 and 2030 technology; and monthly Carbon Footprint impacts for the CCH15P system (d), SCHP15 alternative (e), and SPCHC15 alternative (f). Total Primary Energy incorporates all fuel energy extracted to satisfy production by each system, including energy inputs to extraction, transmission/extraction losses, and energy embodied in infrastructure.

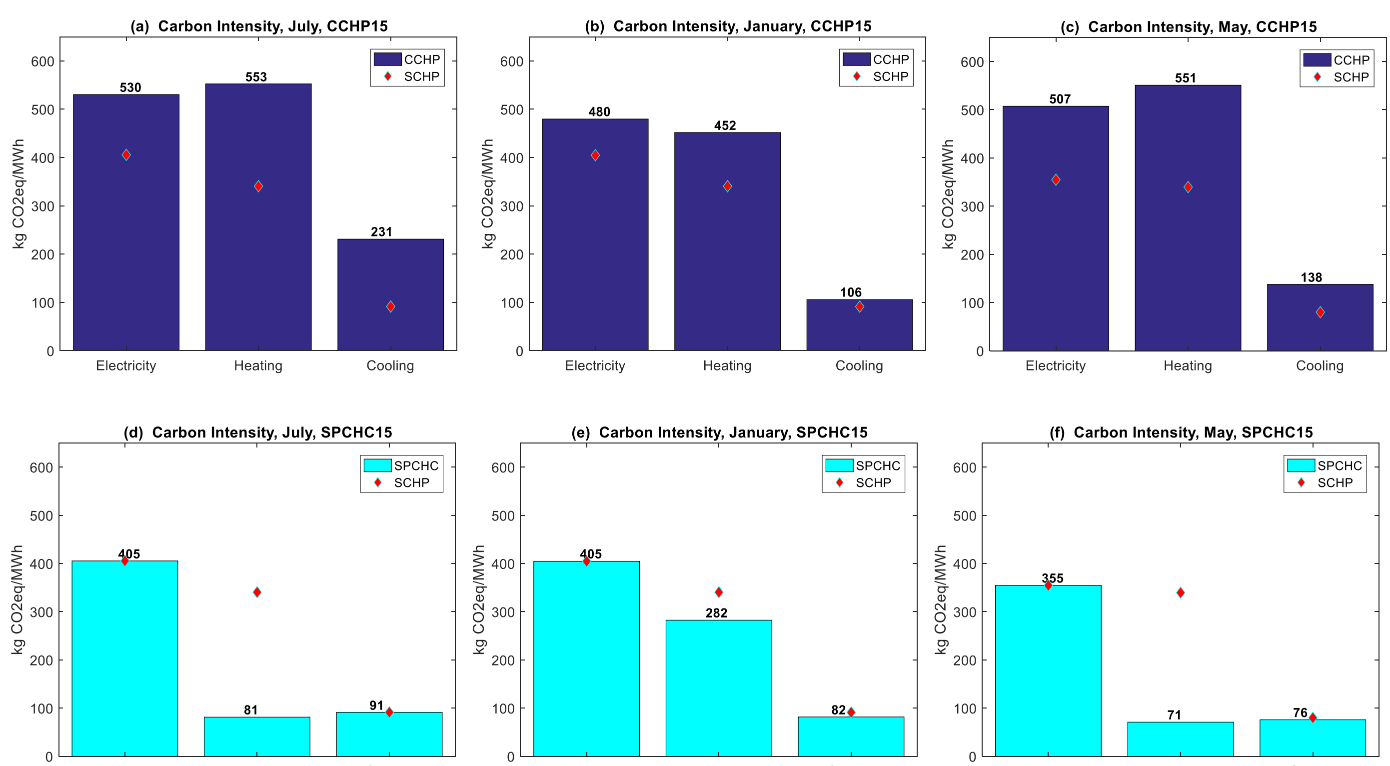

Fig. 5. Carbon intensities of electricity, heating, and cooling for the CCHP (a-c) and SPCHC (d-f) systems, in a cooling season (July), heating season (January), and a shoulder season (May). Diamond markers represent the carbon intensities for the SCHP system, which can differ monthly due to monthly grid mix variations.

Table 1
Technological parameters and average ISO-NE grid mix for 2015, 2030.

Scenario Parameters	2015 average	2015 marginal	2030
Local system parameters			
Chiller Coefficient of Performance (COP)	4.7	4.7	7
Heat Recovery Chiller COP	5.6	5.6	5.6
Boiler Annual Fuel Use Efficiency (AFUE)	0.85	0.85	0.90
Steam distribution losses	15%	15%	10%
CHP Gas turbine electrical efficiency	0.295	0.295	0.357
CHP Gas turbine thermal efficiency	0.35	0.35	0.43
CCHP BOP losses (2015 = 1)	1	1	0.7
ISO-NE Grid Mix*			
Natural Gas	48.5%	74.2%	59.7%
Nuclear	29.9%	0%	18.6%
Coal	3.3%	3.1%	1.4%
Oil	1.9%	4.7%	0.4%
Wind	2.1%	0%	12.0%
Solar	0.4%	0%	1.4%
Hydro	7.5%	1%	5.0%
Other Renewables	6.5%	0.6%	1.5%
Pumped Storage	0%	16.5%	0%
ISO-NE fossil plant thermal efficiency			
Natural Gas	43.3%	43.3%	44.6%
Coal	32.5%	32.5%	32.5%
ISO-NE carbon intensity ($kgCO_{2eq}$/MWh)	376	625	391

**In the 2015 analysis monthly grid mix is used [59], the average annual contribution of technologies is shown here. Monthly data is shown in the Appendix. The 2030 grid mix is estimated from ISO-NE forecasts [60–62]. 'Other Renewables' includes biomass and waste, but is treated as biomass only in our calculations. Efficiencies are based on lower heating value.*

shoulder season month with comparably sized heating and cooling loads (May). Intensities of grid electricity and separate heating and cooling in the SCHP15 system are marked by red diamonds for comparison. These vary monthly due to variations in grid electricity mix. We see that in each month electricity, heating, and cooling are all produced with a higher carbon intensity by the current CCHP15 system than with separate production[4] (Fig. 5a – c). Carbon intensities of heating, cooling, and electricity in the CCHP15 are smallest in colder months due to greater utilization of HRSG steam, free ambient cooling and smaller BOP use/losses.

Further intensity reductions for heating and cooling are achievable by cogenerating hot and cold water in a HRC (Fig. 5d – f). Heating intensities are lowest in warmer months (Fig. 5d and f) when cooling demand is high enough to allow all of the heating demand is to be supplied by the HRC, requiring no natural gas combustion. On the other hand, in winter when heating loads outstrip cooling loads (Fig. 5e), there is insufficient hot water generation from the HRC to meet total heating demand, and heat production is supplemented by regular gas boilers. Although the HRC could still run when cooling demand is low and instead extract heat from a ground source, this possibility was not included in the present analysis. We see in Fig. 5 how a changing grid mix affects the carbon intensities of grid electricity and electric powered heating/cooling. Carbon intensities for cooling, heating, and electricity for each month of 2015 are summarized in Table A7 and annual average energy and environmental impact intensities are shown in Fig. A6.

5. Discussion

5.1. Interpretation

The results presented above describes a case where, by a number of energy and environmental metrics, cogeneration of heat and electricity with periodic use of excess steam for compression cooling is neither preferable to grid electricity and separate generation of heating and cooling, nor to grid electricity and cogeneration of heating and cooling with thermal energy storage. These results may seem unintuitive, as one might expect the utilization of waste heat in CHP to make it more efficient than other alternatives, particularly separate heat and power. Why then do the results tell a different story? The primary energy results are firstly dependent on the efficiency of grid electricity and standalone heat, as compared to CHP. This comparison has changed considerably in the past decade or two, so that a 33% efficient thermal power plant is no longer a valid reference case, at least in the US. Such an efficiency is representative of average US coal power plants [54], but in many parts of the US natural gas has replaced or is replacing coal as the dominant source of grid electricity, and the average efficiency of 43% for natural gas electricity is growing, albeit slowly, as newer plants come online [54]. The global average efficiency of CHP meanwhile was 59% in 2016 [64]. Different fuel inputs, BOP use, transmission and distribution losses, and levels of heat utilization complicate such comparisons and are case specific. In this case study the primary energy requirements for electricity and heating (without cooling) show little difference between systems based on CHP and separate production (i.e. CCHP15 vs SCHP15) with current efficiency, while CCHP system requires less primary energy for electricity and heating under assumptions about more efficient production in 2030.

The relatively close comparison of primary energy requirements between CCHP and alternatives in this case study does not carry over to comparisons of GHG emissions or other environmental impacts. We show how efficiency improvements to the CCHP system in 2030 makes its primary requirements smaller than SCHP30, yet due to the types of input energy this does not translate into carbon benefits. Crucially, as grid electricity incorporates more low carbon generation sources, the GHG benefits of CHP will reduce, while the benefits of electrified and combined heating and cooling will increase. That is exactly what we find in this study, situated in the Northeast US, but this is clearly a regionally specific issue. We can

[4] One exception to this is in February, when due to much higher inputs of coal and oil than average, grid electricity has a higher carbon intensity than electricity from the CHP system.

conclude that the energy and carbon benefits of CHP depend on a number of site specific criteria, most importantly:

- The efficiency and carbon intensity of regional grid electricity
- The efficiency and carbon intensity of power and heat from the CHP system
- The efficiency and carbon intensity of independent heat production via boilers, furnaces, heat pump, or other alternatives
- Transmission, distribution, and BOP losses
- The relative size over short time spans (hours-days) and seasonal variations of heating and power demands
- The capacity for thermal energy storage

The last two points determine utilization of heat from CHP, which in turn influences the effective efficiency and environmental intensities of CHP heat. While our data do not facilitate analysis of time steps shorter than one month, dynamic ratios of heating, cooling, and electricity demands can result in different optimal operation configurations of polygeneration systems. The generation priority (i.e. electric vs thermal load following) and ability to respond quickly to changes in demand can greatly affect heat utilization, waste and overall system efficiency. Other options to increase heat utilization, such as absorption chillers/heat pumps, were not considered in this analysis. Adding in cooling to the analysis, and if cogeneration of heating and cooling is feasible, some additional factors become relevant:

- The efficiency (COP) of independent chillers and HRC
- The relative magnitudes and variation of cooling, heating, and power demands

The above criteria echo and add to Espirito Santo's primary energy related factors for determining the feasibility of trigeneration systems – "(i) grid thermal plant efficiency; (ii) hot water and steam production efficiency; (iii) electrical chiller efficiency; and, of course, (iv) cogeneration efficiency" [65].

5.2. Viability of combined heat and power

Identifying the determinants of CHP or CCHP benefits is a necessary first step in designing systems for minimum environmental impact. An improvement on this would be to add some numbers to these criteria to aid in system selection. To this end we demonstrate a heuristic developed for determining when CHP is preferable to independent heat and power generation from a GHG mitigation perspective. Fig. 6 shows a viability space (the white area) for which gas-fired CHP can reduce total system GHG emissions over a range of CHP electrical efficiencies (20%–45%), and grid electricity GHG intensity values (0 – 1,200 $kgCO_2$-eq/MWh). The curved lines, consisting of breakeven points for GHG intensity of grid electricity, are plotted using four combinations of assumed heat utilization and heat recovery rates. If the GHG intensity of grid electricity is lower than the breakeven curves, CHP is not recommended as it does not reduce system GHG emissions. Breakeven points for GHG intensity of grid electricity are found by identifying values of $GHG_{e,grid}$ which satisfy Eq. (6). Total GHG emissions, GHG_{CHP}, from a CHP system generating W_e of electricity with Q_h of heat recovery and utilization are equated with GHG emissions from generating W_e of grid electricity and Q_h of heat from a gas boiler.

$$GHG_{CHP} = GHG_{e,grid} + GHG_{h,b} \tag{6}$$

GHG emissions from the CHP system and gas boiler ($GHG_{h,b}$) are calculated as shown in Eqs. (7) and (8), where $\eta_{e,CHP}$ is the electrical efficiency of the CHP system, C_{ng} is the carbon intensity of combusting 1 MWh heat content of natural gas, η_b is the efficiency of the gas boiler, and Q_h is the amount of heat generated by each system, calculated as the ratio of CHP thermal efficiency, $\eta_{t,CHP}$, to $\eta_{e,CHP}$. We calculate $\eta_{t,CHP}$ by multiplying the maximum amount of heat potentially available for recovery, *(1- $\eta_{e,CHP}$)*, by heat recovery and utilization factors r and u (Eq. (9)). Heat recovery is limited by fuel combustion inefficiencies, heat losses from turbine equipment, and the effectiveness of the heat exchanger (such as a heat recovery steam generator) which can range from 20–85% [66,67]. In the case study the CCHP system heat recovery factor was 50%. Heat utilization can range from 0–100%, depending on time-sensitive supply and demand for heating services, and can be increased by TES.

$$GHG_{CHP} = \frac{C_{ng}W_e}{\eta_{e,CHP}} \tag{7}$$

$$GHG_{h,b} = \frac{C_{ng}Q_h\ W_e}{\eta_b} \tag{8}$$

$$\eta_{t,CHP} = ur(1 - \eta_{e,CHP}) \tag{9}$$

The solution for $GHG_{e,grid}$ simplifies to Eq. (10), which is equivalent to the carbon intensity of electricity in $kgCO_{2eq}$/MWh when W_e is 1 MWh. Calculations are shown in the 'Viability Data' tab of DF-1.

$$GHG_{e,grid} = \frac{C_{ng}W_e}{\eta_{e,CHP}}\left(1 - \frac{\eta_{t,CHP}}{\eta_b}\right) \tag{10}$$

The following assumptions apply:

- Four combinations of heat recovery rate, r and utilization rate, u are considered resulting in combined ur factors of 0.3, 0.4, 0.5, and 0.7, producing total CHP system efficiencies of 44% – 84%
- The gas boiler thermal efficiency $\eta_b = 85\%$
- Direct GHG intensity of natural gas combustion is $C_{ng} = 189$ $kgCO_{2eq}$/MWh, while life cycle intensity is $C_{ng} = 280$ $kgCO_{2eq}$/MWh, incorporating extraction, transport, and combustion.

The breakeven calculations were made using both direct emissions intensities (Fig. 6a), and lifecycle emission intensities (Fig. 6b). 2016 carbon intensities for selected eGrid subregions of US are plotted in the sidebars for comparison. The direct intensities are available from the most recent eGrid summary tables [68], and the lifecycle intensities were calculated in THEMIS based on regional fuel mixes. A number of interpretations can be drawn from Fig. 6. First, levels of heat recovery and utilization are very important and can make a great deal of difference in how CHP compares with independent production. We consider combined ur factors of 0.4 – 0.5 to be a reasonable representation of current CHP systems, while a ur of 0.7 as shown in the lowermost curved line is rather optimistic. Dynamic electricity, heating, and cooling demands generally pose a utilization challenge for co/polygeneration systems, which TES can help address. Second, the trend of the breakeven grid carbon intensities with increasing $\eta_{e,CHP}$ is mildly parabolic, so that efficiency increases in CHP electricity at lower efficiencies (say from 20% to 25%) lead to larger performance improvements than increases at the higher end (e.g. 35%–40%). This means that as higher electrical efficiencies are achieved, it becomes harder to improve the relative benefits of CHP through further efficiency increases. Third, at an electrical efficiency representing high performance meso-level CHP today ($\eta_{el,CHP} = 30$–35%) and a combined utilization-recovery rate of $ur = 0.5$, some US regions (i.e. NYUP, CAMX, NWPP) have electricity of sufficiently low carbon intensity to overturn the GHG benefits of CHP. More regions (e.g. RFCE, SRVC) would find CHP to increase total GHG emissions if considering upstream emissions, or if heat utilization and recovery factors were lower.

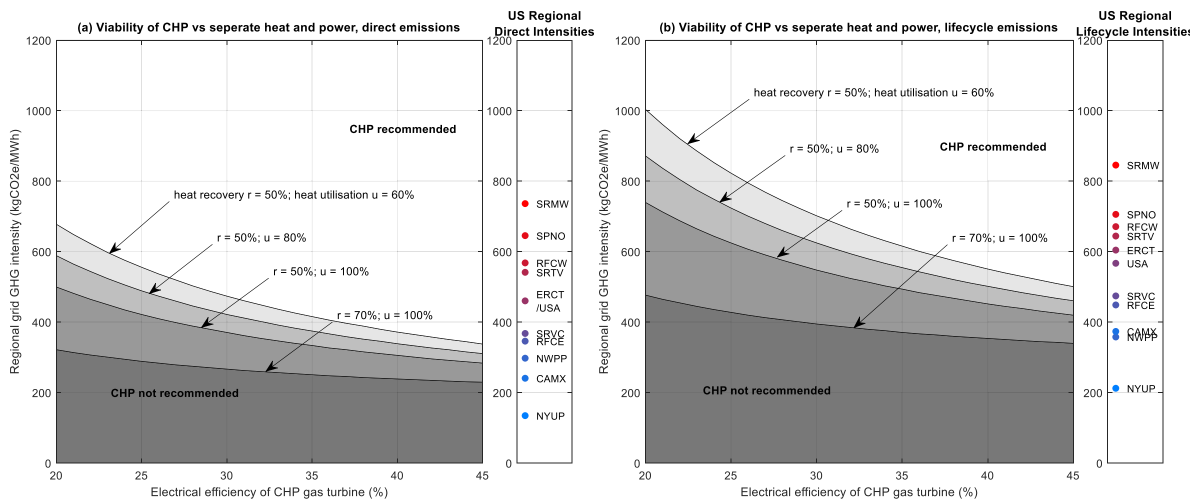

Fig. 6. Viability of CHP under varying electrical efficiency of CHP turbine and GHG intensity of grid electricity with four levels of heat recovery and utilization, based on (a) direct power plant emissions and (b) lifecycle emissions. Side panel indicates direct and lifecycle GHG intensity of selected eGRid subregions [68]: NYUP = Upstate New York, CAMX = California, NWPP = Northwest Power Pool, RFCE = RFC East, SRVC = SERC Virginia/Carolina, USA = US Average, ERCT = ERCOT (Texas), SRTV = SERC Tenn. Valley, RFCW = RFC West, SPNO = SPP North, SRMW = SERC Midwest. See map of eGrid subregions in Fig. A9.

5.3. Limitations

A number of limitations to this study are described to clarify what simplifications have been made, what factors were not considered, and what extensions to this line of analysis are possible in future work. First, a number of benefits of distributed polygeneration systems are not taken into consideration by the lifecycle metrics presented above. Resilience benefits, an increasingly desired component of energy supply and a potential advantage of distributed generation, are not considered. The advantages of consuming energy which is not entirely dependent on centralized generation are numerous. In the case of an outage event due to extreme weather or sabotage, or merely when grid electricity is in high demand and very expensive, or carbon intensive, having capacity to operate an islandable energy supply system is clearly valuable. Many smaller plants do not have this capacity as they lack the necessary controls to provide grid stability. Potential economic benefits of polygeneration systems were also not considered.

Second, academic institutions are a particular type of energy customer with a number of potential avenues for reducing energy consumption and environmental impacts. Capital upgrades such as building efficiency retrofits and new building projects influence total building energy demand, and ideally can be combined and overlap with energy supply strategies to mitigate future environmental impacts while considering capital and operational costs. Such considerations were outside the scope of this study. Third, the monthly inventory data used limits the analysis by neglecting short-term energy supply and demand dynamics. To take advantage of arbitrage opportunities for example, thermal energy (hot and cold), and pumped storage for the grid could be charged at night or other times of low demand when grid electricity is cheaper. Baseload power plants, such as coal and nuclear, may contribute more to these charging hours, influencing the environmental outcomes [69]. In ISO-NE it is possible that a high contribution of nuclear to baseload generation may reduce the carbon intensity of electricity used for off-peak thermal generation and energy storage, but such effects have not been considered here. We consider our marginal grid electricity sensitivity analysis a worst case scenario for grid carbon intensity.

Finally, the environmental benefits of the alternatives presented represents a best case scenario for SPCHC – where the HRC is capable of providing for all simultaneous loads of heating and cooling that are within its generation capacity, due to sufficient TES capacity and no storage losses. An important limitation is that we do not investigate different operating conditions and efficiencies of a HRC run at partial load. Notwithstanding the limitations addressed here, the authors are confident that the results, conclusions, and implications provide valuable insights for energy system researchers, designers, and policymakers.

6. Conclusions

This paper offers ground-truthing of the environmental benefits of district energy polygeneration systems, comparing lifecycle energy and environmental impacts of CHP and combined heating and cooling systems with separate generation of electricity, heating, and cooling for a university campus. Our case study results show that primary energy requirements of CHP and partially steam compressed cooling are slightly higher than separate generation, or slightly lower if efficiencies improve, while combined heating and cooling requires substantially less primary energy. GHG emissions and other environmental impacts on the other hand are found to be much lower from SCHP or SPCHC than from CCHP. Primary energy requirements and environmental impacts of polygeneration systems are heavily dependent on local conditions, particularly thermal and electrical efficiencies, BOP and distribution losses, and fuel inputs to regional electricity. Carbon intensities vary throughout the year, with CHP performing better in winter and combined heating and cooling performing better in summer. While using steam for compressing a refrigeration cycle can increase heat utilization, generating steam in summer months from CHP or direct combustion should be avoided if possible, as electric chillers or heat recovery chillers and grid electricity can deliver cooling and electric power with higher efficiency and lower GHG emissions.

Cogeneration of heating and cooling in a HRC can offer great reductions in primary energy requirements, GHG emissions and other environmental impacts. This motivates further research into increasing uptake of HRC where possible, and a broader shift of what is combined in polygeneration systems, from combined heat-

ing and power to combined heating and cooling. Results are increasingly relevant in light of the need to drastically reduce GHG emissions associated with heating and cooling buildings. The potential of HRC to do exactly that is illustrated in Fig. 5d–f. TES can act as a buffer to maximize utilization of a HRC, and can facilitate purchasing of electricity for thermal generation when grid electricity is cheapest, and/or has low carbon intensity. The same benefits of TES can apply to traditional CHP, but with low-carbon grid electricity, separate production of heat and power will in most cases remain better suited to avoiding GHG emissions than CHP. Additional resilience benefits of distributed energy generation and TES exist but were not explored in this analysis.

Finally, a heuristic which can aid in decisions between CHP and independent generation for a general case based on CHP efficiency and regional carbon intensity is illustrated. This identifies breakeven carbon intensities of regional electricity below which CHP does not deliver GHG emission reductions, and compares these to carbon intensities of selected grid regions in the US.

Acknowledgements

The authors gratefully acknowledge contributions of Yale Power Plant manager Sam Olmstead in providing data and advice regarding the operation of the Yale Power Plant, and Joe Stagner, for consultation on the operation of SESI, the energy production system at Stanford University. We thank Niko Heeren for helpful comments, although we remain responsible for any errors. This research did not receive any specific grant from funding agencies in the public, commercial, or not-for-profit sectors. The authors declare no conflicts of interest.

Appendix

A.1. Grid mixes

Table A1.

Table A1
Monthly Average Generation by Fuel Type, source: [59].

Average Generation by Month 2015								
	Other Ren.	*Wind*	*Solar*	*Hydro*	*Nuclear*	*Gas*	*Coal*	*Oil*
January	7%	2%	0%	9%	31%	37%	11%	3%
February	6.5%	2%	0%	7%	27%	29%	11.5%	17%
March	7%	2.5%	0.5%	7%	34.5%	39.5%	8%	1%
April	6.5%	2.5%	0.5%	12%	32%	45.5%	1%	0%
May	6.5%	2%	0.5%	8%	30%	52%	1%	0%
June	6%	1.5%	0.5%	9.5%	31.5%	51%	0%	0%
July	5.5%	1%	0.5%	6%	27.5%	56.5%	2%	1%
August	6%	1%	0.5%	4.5%	27%	60%	1%	0.5%
September	6.5%	1.5%	0.5%	4.5%	30.5%	54.5%	1%	1%
October	7%	3.5%	0.5%	7%	19%	60%	3%	0%
November	7%	3.5%	0.5%	7.5%	29%	49%	3.5%	0%
December	7%	2.5%	0.5%	9%	34.5%	43.5%	2.5%	0.5%

A.2. Scenario parameters

Table A2.

This section describes data and decisions behind the scenario definition summarised in Table 1 of the main manuscript. The 2030 scenario is based upon what we expect to become standard technology by 2030, not best available technology. Average system efficiency worldwide for cogeneration of heat and power is 59%, compared with 43% for electricity generation [64], but state of the art CHP plants can approach 90% [17]. We believe the current CHP system consisting of a gas turbine and HRSG with a total efficiency of 65% to be close to the current state of the art for this capacity of gas turbine (8 MW_{el}), but higher efficiencies can currently be achieved with slightly higher capacity units (see for example the range of turbines from Caterpillar Solar [70]). For future oriented scenarios we contend that higher efficiencies would be feasible even at this scale of generation. We define the efficiency of electric generation from a similar CHP system in 2030 to be 35.7%, a slight improvement on the 34.3% efficient Taurus 70 gas turbine, the most efficient of the Caterpillar Solar turbines in the 8MW_{el} range. We project an improvement in heat recovery and utilization by the HRSG, from 35% to 43%, bringing overall CHP system efficiency to almost 80%.

Table A2
Percentage of time fuel types were marginal each month, source: [59].

Contribution to Monthly Marginal Generation by Month 2015						
	Other Ren	*Hydro*	*Pump Stor.*	*Gas*	*Coal*	*Oil*
January	1%	2.5%	17%	57.5%	14%	8.5%
February	0%	1%	17%	39.5%	4%	39%
March	0.75%	0.75%	29.5%	58%	8%	3%
April	0.5%	1%	17%	81%	0.5%	0%
May	0%	0%	14%	85%	0%	1%
June	0%	1%	16%	83%	0%	0%
July	0.5%	0.5%	15.5%	81%	1.5%	1%
August	1%	1.5%	17%	78.5%	1%	1%
September	0.5%	0.5%	15%	80%	1%	3%
October	1%	0.5%	13%	83%	2.5%	0%
November	0.75%	0.75%	15.5%	79.5%	3.5%	0%
December	1%	2%	11%	84%	2%	0%

For compression chillers, achieving an average COP of 7 (equivalent to 0.5 kW/ton-Refrigeration) is feasible with some of the most efficient equipment today (e.g. [71]), and we consider that to be representative of a feasible average COP for 2030. For distribution losses in the CCHP system, we expect that a future steam loss from distribution of 10% to be reasonable, while we project no improvement in the distribution losses of hot and chilled water. Reflecting systemic performance improvements of the CHP plant, we project BOP consumption of steam, electricity, and chilled water to be 70% of today's levels in 2030.

2030 fuel mix for ISO-NE electricity is based on planned capacity extensions and retirements throughout the ISO-NE region [60,61]. New capacity will be primarily natural gas and wind, while retirements of nuclear, coal, and oil capacity are expected [62]. Calculation of the 2030 grid mixes can be seen in the 'ISONE Gen Mixes' tab of DF-1.

A.3. Lifecycle impact intensities

In Fig. 5 of the main manuscript carbon intensities for selected months are displayed, showing how intensities can be quite different at different times of the year. To give a higher level comparison for more impact types, annual average energy, carbon, particulate matter and freshwater ecotoxicity intensities for 2015 and 2030 scenarios are shown in Fig. A6 (a – d). These intensities incorporate total direct and indirect emissions over the course of the whole year, divided by total consumption of each energy stream over the whole year.

A.4. Marginal impacts

Total annual impacts for 2015 are recalculated based on monthly marginal ISO-NE electricity mix, and are shown here in relation to impacts based on monthly average electricity mix Fig. A7 (a–d). Impacts using marginal electricity mix are marked with an 'm' at the end of the technology-scenario label (e.g. CCHP15m).

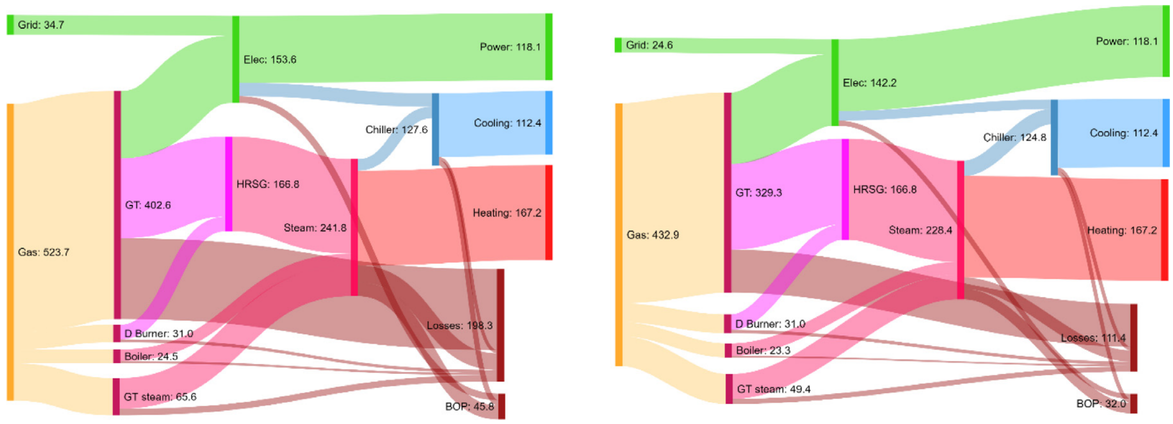

Fig. A1. Sankey diagram of system energy flows for CCHP15 (left) and CCHP30 (right). Unit: GWh.
BOP = Balance of Plant; HRSG = Heat Recovery Steam Generator; GT = Gas Turbine; D Burner = Duct Burner.

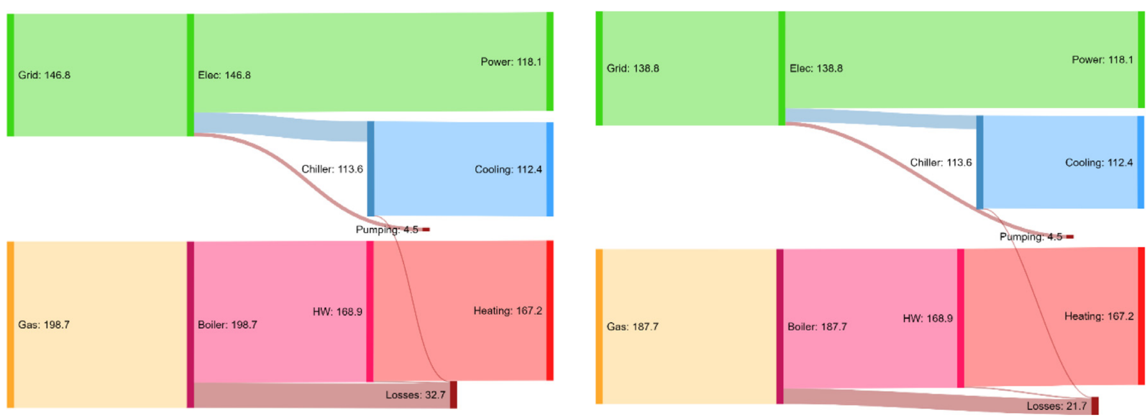

Fig. A2. Sankey diagram of system energy flows for SCHP15 (left) and SCHP30 (right). Unit: GWh
HW = Hot Water.

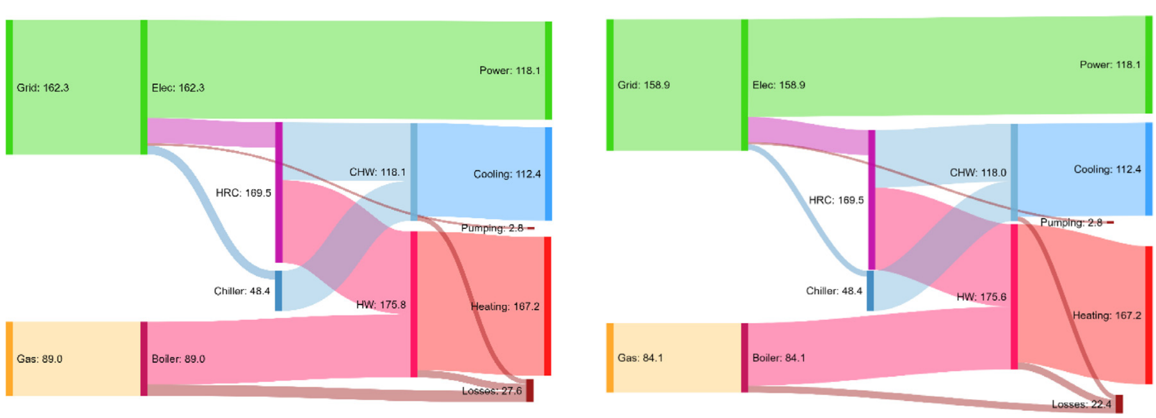

Fig. A3. Sankey diagram of system energy flows for SPCHC15 (left) and SPCHC30 (right). Unit: GWh
HW = Hot Water; CHW = Chilled Water; HRC = Heat Recovery Chiller.

While primary energy requirements are almost the same, the other environmental indicators calculated show higher impacts resulting from the marginal grid electricity. Using marginal electricity, carbon footprint reductions by switching from CCHP to SCHP and SPCHC are 12% (rather than 30%) and 24% (rather than 45%) respectively. Impact reductions shown based on these marginal grid mixes can be thought of as short term marginal impacts. The longer term marginal effects of an increase in demand will include additions to grid capacity, which would contain possibly no coal or oil, and more natural gas and solar PV [60,61].

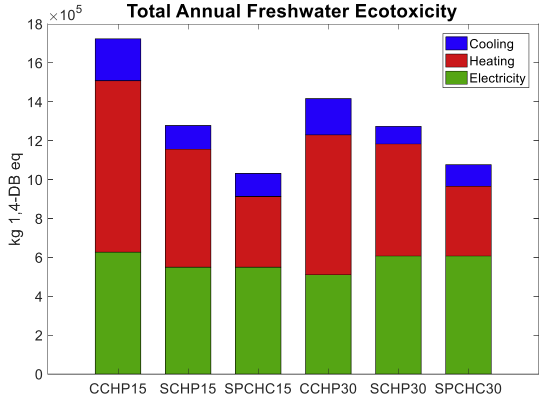

Fig. A4. Total FET Impacts.

A.5. Exergy-allocation of joint production

A sensitivity analysis is performed regarding the allocation procedure for joint production processes. In the main analysis all products of join production processes are allocated impacts based on the energy content of the products. In this sensitivity, allocation was based on the exergy content B of products. Just two processes in any of the technology systems are modelled as joint production processes; the gas turbine and HRSG system of CCHP where both electricity and steam are produced, and the HRC of SPCHC which produces heating and cooling outflows. For those two technology systems, impacts are recalculated using exergy based allocation assuming 2015 technology.

To calculate the exergy content of products, the thermal flows are considered here to have finite mass, rather than being infinite hot or cold reservoirs. The formulations for the exergy of finite hot and cold matter are reproduced from Chapter 36.4 of Jaffe and Taylor [72]

$$B_{hot\ \ matter} = c\left(T - T_{ref}\right)\left(1 - \frac{\ln\left(T/T_{ref}\right)}{T/T_{ref} - 1}\right) \tag{A1}$$

$$B_{cold\ \ matter} = c\left(T_{ref} - T\right)\left(\frac{\ln\left(T_{ref}/T\right)}{1 - \ T/T_{ref}} - 1\right) \tag{A2}$$

where c is the constant heat capacity (of water in this case), T is the temperature of the hot or cold matter, and T_{ref} is the reference temperature. These formulations are used for the hot and cold water products of the HRC, as the assumption of constant heat capacity is acceptable for liquid water. The temperature of hot water produced from the HRC is assumed to be 343 K, and the temperature of cold water is assumed to be 279 K. For the gas turbine and HRSG system in CCHP, the pressure and temperature of steam produced are not known with enough certainty to calculate its heat capacity, and therefore the exergy of hot matter is calculated using the relation of exergy of hot matter to exergy of a hot reservoir as depicted in Fig. 36.2b of [72]. A temperature of 423 K is assumed for the saturated steam, at which the ratio of T/T_{ref} is approximately 1.5, corresponding to a $B_{matter}/B_{reservoir}$ ratio of 0.55. The exergy that would be associated with the hot steam if it were an infinite reservoir is thus multiplied by a factor of 0.55. For all exergy calculations, monthly average temperature is taken as the reference temperature [44], reflecting the monthly variations in the reference state. Exergy based calculations and inventories can be found in Data File 3.

Fig. A8a–b demonstrate the difference made by using energy and exergy based allocation. As electricity has much higher exergy than the steam produced by the HRSG, impacts from electricity increase a lot in the CCHP15 system; primary energy requirements associated with electricity increase by 67%, and carbon footprint impacts by 72%, bringing the implied average carbon intensity of electricity to 880 kg-$CO_{2\text{-eq}}$/kWh. In the SPCHC systems, exergy allocation increases slightly the impacts from heating and reduces those from cooling. This is because the heating flows have greater temperature difference with the reference temperature, resulting in higher exergy values. Comparing Fig. A8c–d with corresponding Figs. 4d and A5a demonstrate at a monthly level how impacts are distributed.

A.6. Regional electricity GHG Intensities

Direct GHG intensities of regional electricity is taken from eGrid summary tables [68], reflecting 2016 generation mixes and emissions. Fuel mixes are transmission losses data are used in THEMIS to calculate life cycle GHG emission intensities. The map of eGrid subregions of the contiguous USA is shown in Fig. A9.

A.7. Impact summary tables

Tables A3–A6 summarise impacts related to demand for electricity, heating, and cooling, for the three alternatives under standard technology in 2015 and 2030, with sensitivities based on using marginal electricity, and exergy based allocation, in 2015. Impacts are shown for the primary energy requirements, carbon footprint (GHG emissions), particulate matter, and freshwater ecotoxicity.

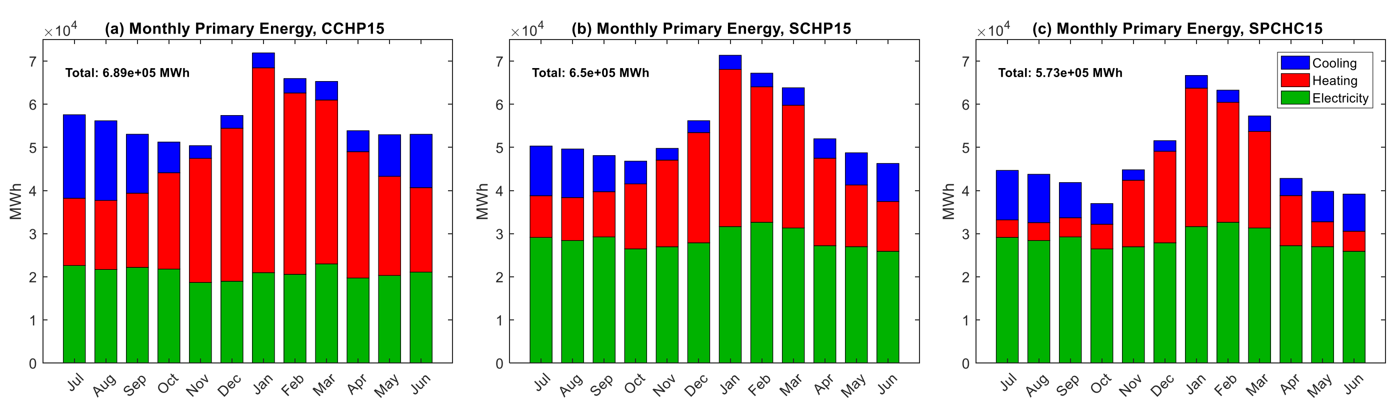

Fig. A5. Monthly Primary Energy Requirements for CCHP (a), SCHP (b), and SPCHC (c).

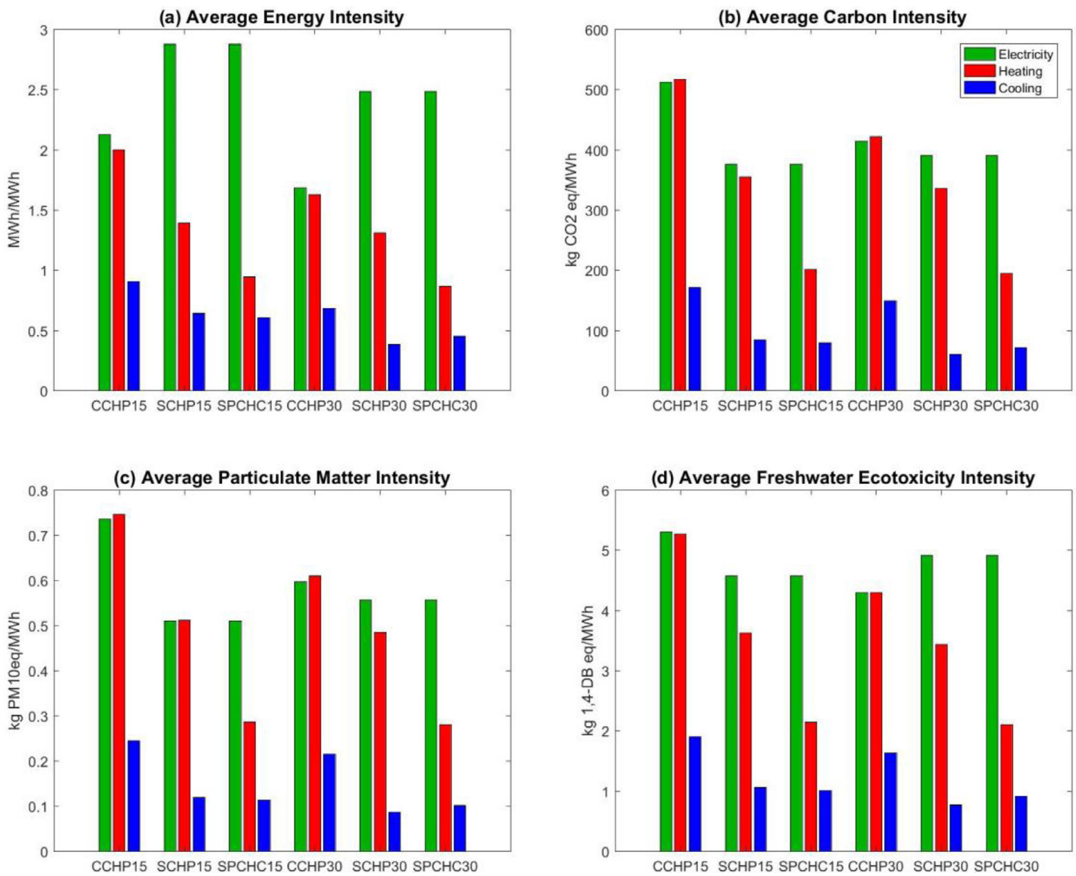

Fig. A6. Annual average impact intensities for 2015 and 2030.

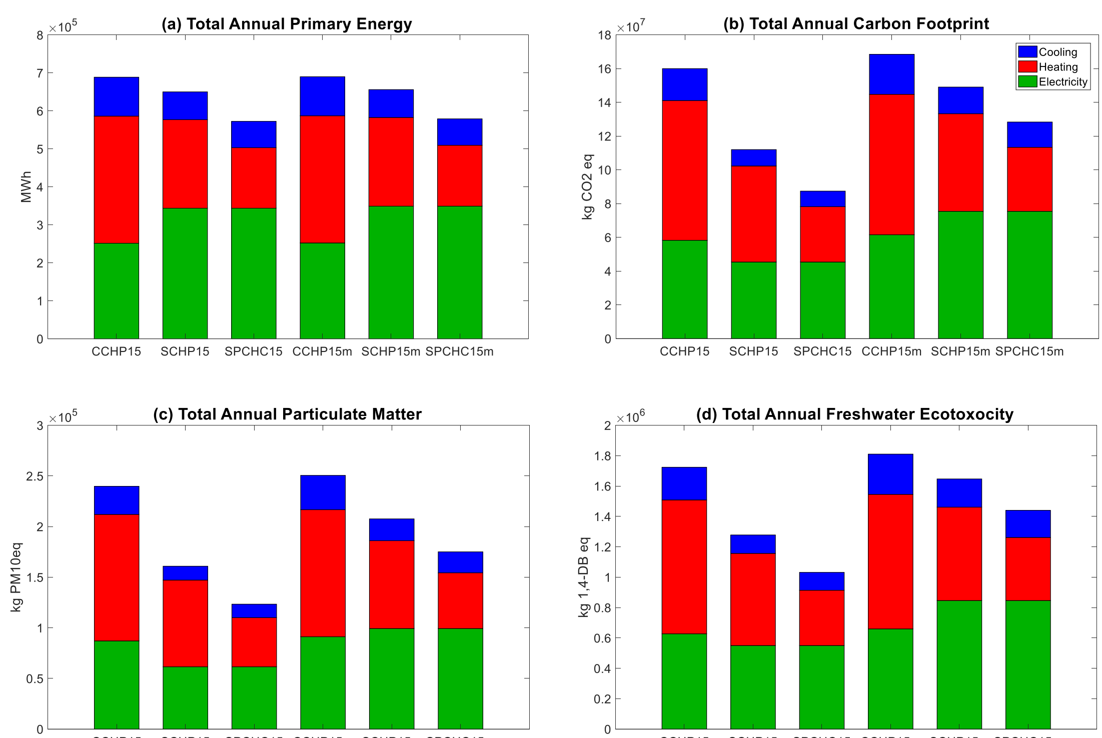

Fig. A7. Impacts calculated with 2015 average monthly electricity (left) mix and 2015 marginal electricity mix (right).

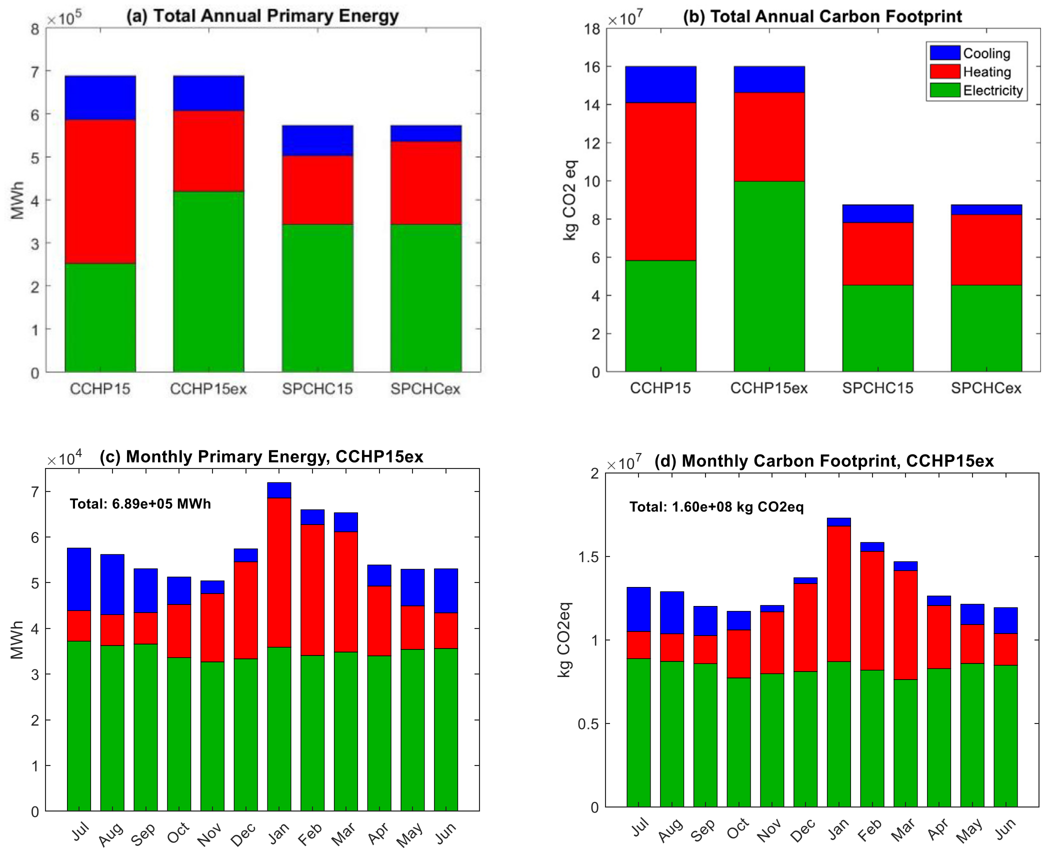

Fig. A8. Annual (a-b) and Monthly (c-d) Primary Energy and Carbon Footprint impacts for 2015 scenario with exergy allocation applied to joint production processes.

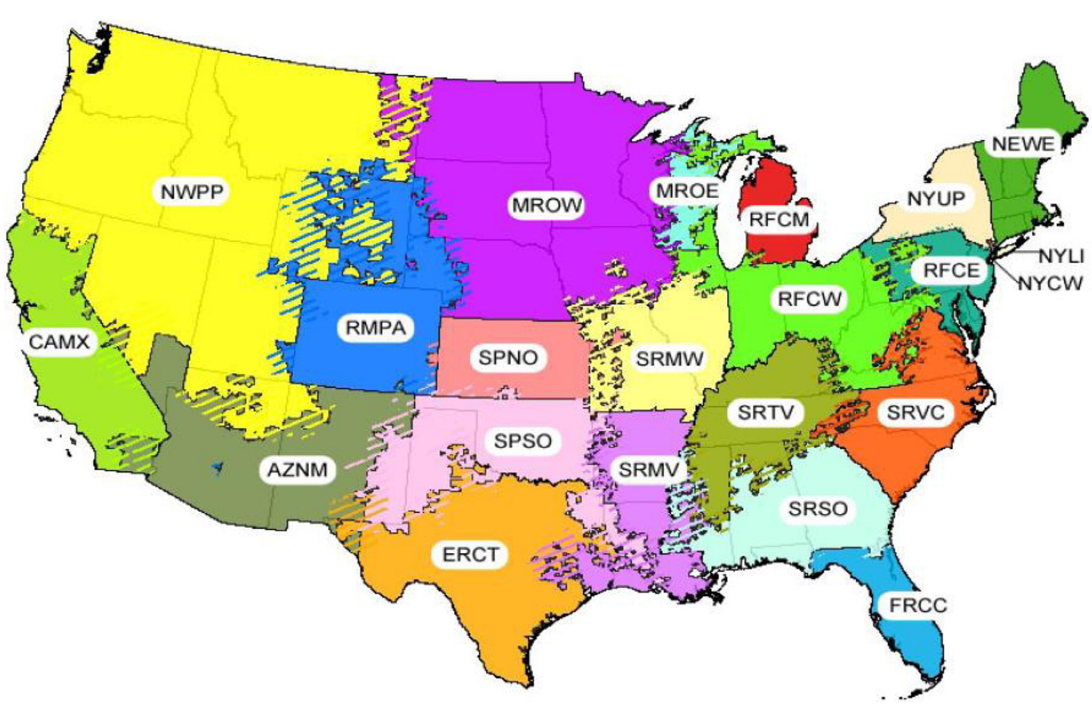

Fig. A9. Map of eGrid Subregions, adapted from [68].

Table A3
Summary of Primary Energy Requirements (Cumulative Energy Demand) for each technology and scenario.

Cumulative Energy Demand Impacts (GWh)				
Tech-Scenario	*Electricity*	*Heating*	*Cooling*	*Total*
CCHP15	252	335	102	689
CCHP15m	252	335	103	690
CCHP15ex	419	188	81	689
CCHP30	200	272	77	550
SCHP15	344	233	73	650
SCHP15m	349	233	73	656
SCHP30	304	220	45	568
SPCHC15	344	159	69	573
SPCHC15m	349	160	70	579
SPCHC15ex	344	191	37	573
SPCHC30	304	147	53	504

Table A4
Summary of Carbon Footprint Impacts for each technology and scenario.

Carbon Footprint Impacts (kton CO_2-eq)				
Tech-Scenario	*Electricity*	*Heating*	*Cooling*	*Total*
CCHP15	58.3	82.8	18.9	160
CCHP15m	61.5	83.2	23.7	168
CCHP15ex	99.8	46.6	13.6	160
CCHP30	47.2	67.6	16.5	131
SCHP15	45.4	56.9	9.7	112
SCHP15m	75.4	57.8	15.8	149
SCHP30	48.6	53.9	7.1	110
SPCHC15	45.4	32.8	9.2	87
SPCHC15m	75.4	37.9	15.0	128
SPCHC15ex	45.4	37.0	5.0	87
SPCHC30	48.6	32.0	8.5	89

Table A5
Summary of Particulate Matter Impacts for each technology and scenario.

Particulate Matter Impacts (ton PM10-eq)				
Tech-Scenario	*Electricity*	*Heating*	*Cooling*	*Total*
CCHP15	87.1	124.9	27.8	240
CCHP15m	91.2	125.4	33.9	251
CCHP15ex	149.8	70.2	19.8	240
CCHP30	70.8	102.0	24.5	197
SCHP15	61.5	85.6	13.7	161
SCHP15m	99.3	86.7	21.6	208
SCHP30	69.2	81.2	10.2	161
SPCHC15	61.5	48.5	13.3	123
SPCHC15m	99.3	55.0	20.7	175
SPCHC15ex	61.5	54.3	7.5	123
SPCHC30	69.2	47.8	12.4	129

Table A6
Summary of Freshwater Ecotoxicity Impacts for each technology and scenario.

Freshwater Ecotoxicity Impacts (ton 1,4-DB eq)				
Tech-Scenario	*Electricity*	*Heating*	*Cooling*	*Total*
CCHP15	626	881	214	1721
CCHP15m	658	885	262	1805
CCHP15ex	1068	496	157	1721
CCHP30	508	719	184	1411
SCHP15	540	606	119	1266
SCHP15m	830	614	182	1626
SCHP30	581	575	87	1243
SPCHC15	540	359	113	1012
SPCHC15m	830	409	172	1411
SPCHC15ex	540	411	61	1012
SPCHC30	581	352	103	1035

Table A7
Summary of Carbon Intensities for 2015 scenarios.

Carbon Intensities (kg CO_2-eq/MWh)									
	Electricity			*Heating*			*Cooling*		
	CCHP15	*SCHP15*	*SPCHC15*	*CCHP15*	*SCHP15*	*SPCHC15*	*CCHP15*	*SCHP15*	*SPCHC15*
July	530	405	405	553	341	81	231	91	91
Aug	525	406	406	550	341	81	223	91	91
Sept	510	382	382	561	340	77	219	86	84
Oct	481	427	427	507	341	85	157	96	88
Nov	467	363	363	495	340	233	98	82	74
Dec	467	324	324	480	339	257	90	73	66
Jan	480	405	405	452	341	282	106	91	82
Feb	492	524	524	466	343	288	132	118	105
Mar	455	364	364	461	340	236	97	82	73
Apr	474	314	314	498	339	144	87	71	63
May	507	355	355	551	340	71	138	80	76
June	533	337	337	578	339	68	160	76	74

References

[1] California environmental protection agency, 2015. Climate change research plan for California http://climatechange.ca.gov/climate_action_team/reports/CAT_research_plan_2015.pdf.

[2] NYC mayor's office of sustainability, 1.5 °C: Aligning New York City with the Paris climate agreement, New York, 2017. http://www1.nyc.gov/site/sustainability/codes/1.5-climate-action-plan.page.

[3] K. Gillingham, S. Carattini, D. Esty, Lessons from first campus carbon-pricing scheme, Nature 551 (2017) 27–29, doi:10.1038/551027a.

[4] IEA, 2017. Key world energy statistics 2017, Paris https://www.iea.org/publications/freepublications/publication/KeyWorld2017.pdf.

[5] IEA, World Energy Balances, in: IEA World Energy Stat. Balanc., 2017.

[6] IPCC, Mitigation of climate change, Contribution of Working Group III to the Fifth Assessment Report of the Intergovernmental Panel on Climate Change, Cambridge Univ. Press, Cambridge, UK New York, NY, 2014, doi:10.1017/CBO9781107415416.

[7] A. Eisentraut, B. Adam, Heating Without Global Warming, International Energy Agency, Paris, 2014.

[8] J.M. Cullen, J.M. Allwood, The efficient use of energy: tracing the global flow of energy from fuel to service, Energy Policy 38 (2010) 75–81, doi:10.1016/j.enpol.2009.08.054.

[9] V.P. Shah, D.C. Debella, R.J. Ries, Life cycle assessment of residential heating and cooling systems in four regions in the United States, Energy Build 40 (2008) 503–513, doi:10.1016/j.enbuild.2007.04.004.

[10] B. Güneralp, Y. Zhou, D. Ürge-Vorsatz, M. Gupta, S. Yu, P.L. Patel, M. Fragkias, X. Li, K.C. Seto, Global scenarios of urban density and its impacts on building energy use through 2050, Proc. Natl. Acad. Sci. 114 (2017) 201606035, doi:10.1073/pnas.1606035114.

[11] S. Beucker, J.D. Bergesen, T. Gibon, Building energy management systems: global potentials and environmental implications of deployment, J. Ind. Ecol. 20 (2016) 223–233, doi:10.1111/jiec.12378.

[12] L. Yang, R. Zmeureanu, H. Rivard, Comparison of environmental impacts of two residential heating systems, Build. Environ. 43 (2008) 1072–1081, doi:10.1016/j.buildenv.2007.02.007.

[13] D. Cespi, F. Passarini, L. Ciacci, I. Vassura, V. Castellani, E. Collina, A. Piazzalunga, L. Morselli, Heating systems LCA: Comparison of biomass-based appliances, Int. J. Life Cycle Assess. 19 (2014) 89–99, doi:10.1007/s11367-013-0611-3.

[14] M. Prek, Environmental impact and life cycle assessment of heating and air conditioning systems, a simplified case study, Energy Build 36 (2004) 1021–1027, doi:10.1016/j.enbuild.2004.06.008.

[15] I. Blom, L. Itard, A. Meijer, LCA-based environmental assessment of the use and maintenance of heating and ventilation systems in Dutch dwellings, Build. Environ. 45 (2010) 2362–2372, doi:10.1016/j.buildenv.2010.04.012.

[16] G. Chicco, P. Mancarella, Distributed multi-generation: a comprehensive view, Renew. Sustain. Energy Rev. 13 (2009) 535–551, doi:10.1016/J.RSER.2007.11.014.

[17] IEA, Linking Heat and Electricity Systems, Paris, 2014.

[18] A. Rong, Y. Su, Polygeneration systems in buildings: a survey on optimization approaches, Energy Build. (2017), doi:10.1016/j.enbuild.2017.06.077.

[19] M. Ameri, Z. Besharati, Optimal design and operation of district heating and cooling networks with CCHP systems in a residential complex, Energy Build. (2016), doi:10.1016/j.enbuild.2015.10.050.

[20] P.J. Mago, L.M. Chamra, Analysis and optimization of CCHP systems based on energy, economical, and environmental considerations, Energy Build 41 (2009) 1099–1106, doi:10.1016/j.enbuild.2009.05.014.

[21] K.M. Powell, J. Suk, W.J. Cole, K. Kapoor, J.L. Mojica, J.D. Hedengren, T.F. Edgar, Thermal energy storage to minimize cost and improve efficiency of a polygeneration district energy system in a real-time electricity market, Energy 113 (2016) 52–63, doi:10.1016/j.energy.2016.07.009.

[22] F. Calise, M. Dentice d'Accadia, L. Libertini, E. Quiriti, R. Vanoli, M. Vicidomini, Optimal operating strategies of combined cooling, heating and power systems: a case study for an engine manufacturing facility, Energy Convers. Manag. 149 (2017) 1066–1084, doi:10.1016/j.enconman.2017.06.028.

[23] A. Stoppato, A. Benato, N. Destro, A. Mirandola, A model for the optimal design and management of a cogeneration system with energy storage, Energy Build. (2016), doi:10.1016/j.enbuild.2015.09.036.

[24] H. Ren, W. Zhou, K. Nakagami, W. Gao, Q. Wu, Multi-objective optimization for the operation of distributed energy systems considering economic and environmental aspects, Appl. Energy. 87 (2010) 3642–3651, doi:10.1016/j.apenergy.2010.06.013.

[25] K.C. Kavvadias, Z.B. Maroulis, Multi-objective optimization of a trigeneration plant, Energy Policy. (2010), doi:10.1016/j.enpol.2009.10.046.

[26] M. Carvalho, M.A. Lozano, L.M. Serra, Multicriteria synthesis of trigeneration systems considering economic and environmental aspects, Appl. Energy. 91 (2012) 245–254, doi:10.1016/j.apenergy.2011.09.029.

[27] D. Zhang, S. Evangelisti, P. Lettieri, L.G. Papageorgiou, Optimal design of CHP-based microgrids: multiobjective optimisation and life cycle assessment, Energy 85 (2015) 181–193, doi:10.1016/J.ENERGY.2015.03.036.

[28] A. Osman, R. Ries, Life cycle assessment of electrical and thermal energy systems for commercial buildings, Int. J. Life Cycle Assess. 12 (2007) 308–316, doi:10.1065/lca2007.02.310.

[29] M. Pehnt, Environmental impacts of distributed energy systems-the case of micro cogeneration, Environ. Sci. Policy. 11 (2008) 25–37, doi:10.1016/j.envsci.2007.07.001.

[30] P.J. Mago, A.K. Hueffed, Evaluation of a turbine driven CCHP system for large office buildings under different operating strategies, Energy Build 42 (2010) 1628–1636, doi:10.1016/j.enbuild.2010.04.005.

[31] G. Guest, R.M. Bright, F. Cherubini, O. Michelsen, A.H. Strømman, Life cycle assessment of biomass-based combined heat and power plants: centralized versus decentralized deployment strategies, J. Ind. Ecol. 15 (2011) 908–921, doi:10.1111/j.1530-9290.2011.00375.x.

[32] D. Maraver, A. Sin, F. Sebastián, J. Royo, Environmental assessment of CCHP (combined cooling heating and power) systems based on biomass combustion in comparison to conventional generation, Energy 57 (2013) 17–23, doi:10.1016/j.energy.2013.02.014.

[33] D. Xu, M. Qu, Energy, environmental, and economic evaluation of a CCHP system for a data center based on operational data, Energy Build 67 (2013) 176–186, doi:10.1016/j.enbuild.2013.08.021.

[34] K.A. Kelly, M.C. McManus, G.P. Hammond, An energy and carbon life cycle assessment of industrial CHP (combined heat and power) in the context of a low carbon UK, Energy. 77 (2014) 812–821, doi:10.1016/j.energy.2014.09.051.

[35] Y.Y. Jing, H. Bai, J.-J. Wang, L. Liu, Life cycle assessment of a solar combined cooling heating and power system in different operation strategies, Appl. Energy. 92 (2012) 843–853, doi:10.1109/ICIEA.2012.6360706.

[36] Y. Kikuchi, Y. Kanematsu, R. Sato, T. Nakagaki, Distributed cogeneration of power and heat within an energy management strategy for mitigating fossil fuel consumption, J. Ind. Ecol. 20 (2016) 289–303, doi:10.1111/jiec.12374.

[37] K.K. Roman, J.B. Alvey, Selection of prime mover for combined cooling, heating, and power systems based on energy savings, life cycle analysis and environmental consideration, Energy Build 110 (2016) 170–181, doi:10.1016/J.ENBUILD.2015.10.047.

[38] G. Pagliarini, S. Rainieri, Modeling of a thermal energy storage system coupled with combined heat and power generation for the heating requirements of a University Campus, Appl. Therm. Eng. 30 (2010) 1255–1261, doi:10.1016/j.applthermaleng.2010.02.008.

[39] J.B. Rishel, B.L. Kincaid, Reducing energy costs with condensing boilers & heat recovery chillers, ASHRAE J. 49 (2007) 46–55.

[40] T. Nagota, Y. Shimoda, M. Mizuno, Verification of the energy-saving effect of the district heating and cooling system—simulation of an electric-driven heat pump system, Energy Build 40 (2008) 732–741, doi:10.1016/J.ENBUILD.2007.05.007.

[41] A. Maccarini, M. Wetter, A. Afshari, G. Hultmark, N.C. Bergsøe, A. Vorre, Energy saving potential of a two-pipe system for simultaneous heating and cooling of office buildings, Energy Build 134 (2017) 234–247, doi:10.1016/J.ENBUILD.2016.10.051.

[42] Average Monthly Bill - Residential, Electr. Power Sales, Revenue, Energy Effic. Form EIA-861 Detail. Data Files. (2017), 2016 (accessed April 1, 2018). https://www.eia.gov/electricity/sales_revenue_price/pdf/table5_a.pdf.

[43] P. Berrill, Research data for "Ground truthing the environmental benefits of a polygeneration system: when to combine heat and power? Mendeley Data (2018), doi:10.17632/b8yxrp8d9p.1.

[44] NOAA, 2017. Data Tools: Find a Station (accessed September 1, 2017) https://www.ncdc.noaa.gov/cdo-web/datatools/findstation .

[45] T. Gibon, R. Wood, A. Arvesen, J.D. Bergesen, S. Suh, E.G. Hertwich, A methodology for integrated, multiregional life cycle assessment scenarios under large-scale technological change, Environ. Sci. Technol. 49 (2015) 11218–11226, doi:10.1021/acs.est.5b01558.

[46] R. Frischknecht, J. Niels, 2007. Ecoinvent Rep. No1. 1 http://www.ecoinvent.org/fileadmin/documents/en/01_OverviewAndMethodology.pdf.

[47] B. Weidema, R. Hischier, 2010. ecoinvent data v2.2 www.ecoinvent.org.

[48] A. Burnham, J. Han, C.E. Clark, M. Wang, J.B. Dunn, I. Palou-Rivera, Life-cycle greenhouse gas emissions of shale gas, natural gas, coal, and petroleum, Environ. Sci. Technol. 46 (2012) 619–627, doi:10.1021/es201942m.

[49] V.Z.R. Goedkoop M.J., R. Heijungs, M. Huijbregts, A. De Schryver, J. Struijs, Recipe 2008, a life cycle impact assessment method which comprises harmonised category indicators at the midpoint and the endpoint level; First edition Report I: Characterisation, 2013. doi:10.2307/2930554.

[50] Cornell sustainable campus, optimize the campus heat distribution system, (2013). http://www.sustainablecampus.cornell.edu/initiatives/upgrading-the-heat-distribution-system (accessed December 11, 2017).

[51] J. Stagner, Efficiency and environmental comparisons: combined heat & power (CHP) separate heat & power (SHP) combined heating & cooling (CHC), 2017. http://sustainable.stanford.edu/sites/default/files/SESI_Efficiency_Environmental_Comparisons.pdf.

[52] G. Phetteplace, Heat Distribution Systems, Philadelphia, 1995.

[53] EIA, How much electricity is lost in transmission and distribution in the United States, (2017). https://www.eia.gov/tools/faqs/faq.php?id=105&t=3 (accessed December 16, 2017).

[54] EIA, Average operating heat rate for selected energy sources, Electr. Power Annu. 2016 (2017). https://www.eia.gov/electricity/annual/html/epa_08_01.html. (accessed July 1, 2017).

[55] R. Frischknecht, Allocation in life cycle inventory analysis for joint production, Int. J. Life Cycle Assess. 5 (2000) 85–95, doi:10.1007/BF02979729.

[56] J.A.M. da Silva, J.J.C.S. Santos, M. Carvalho, S. de Oliveira, On the thermoeconomic and LCA methods for waste and fuel allocation in multiproduct systems, Energy. 127 (2017) 775–785, doi:10.1016/J.ENERGY.2017.03.147.

[57] M.A. Lozano, M. Carvalho, L.M. Serra, Allocation of economic costs in trigeneration systems at variable load conditions, Energy Build. (2011), doi:10.1016/j.enbuild.2011.07.002.

[58] A. Laurent, N. Espinosa, M.Z. Hauschild, LCA of Energy Systems, in: M.Z. Hauschild, R.K. Rosenbaum, S.I. Olsen (Eds.), Life Cycle Assess, Springer, 2018, pp. 633–668, doi:10.1111/jiec.12157.

[59] ISO-NE, 2015. ISO New England Electric Generator Air Emissions Report, 2017 http://www.iso-ne.com/%5Cnpapers2://publication/uuid/C5325F32-1AA2-4A38-9E8E-CB0C79C0940B.

[60] ISO-NE, 2017. Resource Mix (accessed July 19, 2017) https://www.iso-ne.com/about/key-stats/resource-mix.

[61] ISO-NE, Integration of renewable resources and other new technologies, 2017 (accessed December 13, 2017). https://www.iso-ne.com/about/regional-electricity-outlook/grid-in-transition-opportunities-and-challenges/integration-of-new-technologies.

[62] ISO-NE, State of the Grid, 2017. 2017 https://www.iso-ne.com/static-assets/documents/2017/01/20170130_stateofgrid2017_presentation_pr.pdf.

[63] N.L. Truong, A. Dodoo, L. Gustavsson, Effects of energy efficiency measures in district-heated buildings on energy supply, Energy 142 (2018) 1114–1127, doi:10.1016/j.energy.2017.10.071.

[64] IEA, Electricity information 2016, IEA Stat. (2016) 1–666.

[65] D.B. Espirito Santo, Energy and exergy efficiency of a building internal combustion engine trigeneration system under two different operational strategies, Energy Build. 53 (2012) 28–38, doi:10.1016/j.enbuild.2012.06.014.

[66] N. Ravi Kumar, K. Rama Krishna, A.V. Sita Rama Raju, Thermodynamic analysis of heat recovery steam generator in combined cycle power plant, Therm. Sci. 11 (2007) 143–156, doi:10.2298/TSCI0704143R.

[67] M. Nadir, A. Ghenaiet, Thermodynamic optimization of several (heat recovery steam generator) HRSG configurations for a range of exhaust gas temperatures, Energy. 86 (2015) 685–695, doi:10.1016/j.energy.2015.04.023.

[68] EPA, 2016. eGRID Summary Tables(2018) https://www.epa.gov/energy/egrid-summary-tables.

[69] M.T. Craig, P. Jaramillo, B.-M. Hodge, Carbon dioxide emissions effects of grid-scale electricity storage in a decarbonizing power system, Environ. Res. Lett. 13 (2018) 14004, doi:10.1088/1748-9326/aa9a78.

[70] Solar Turbines Inc., 2017. Gas Turbine Packages (accessed December 13, 2017) https://mysolar.cat.com/en_US/products/gas-turbine-overview/gas-turbine-packages.html.

[71] Trane, Environmental Product Declaration Trane Centrifugal Chillers, Centravac Chiller Product Portfolio, 2015.

[72] R.L. Jaffe, W. Taylor, The Physics of Energy, 1st ed, Cambridge University Press, 2018, doi:10.1017/9781107016651.